Biological Journal of the Linnean Society, 2006, **89**, 213–239. With 8 figures

Lineage diversification on an evolving landscape: phylogeography of the California newt, *Taricha torosa* (Caudata: Salamandridae)

SHAWN R. KUCHTA* and AN-MING TAN†

Museum of Vertebrate Zoology, 3101 Valley Life Science Bldg., Berkeley, CA 94720–3160, USA

Received 13 December 2004; accepted for publication 5 December 2005

We used mitochondrial cytochrome *b* sequences (up to 778 bp) and starch gel electrophoresis (45 loci) to examine the phylogeographical history of 39 populations of the California newt, *Taricha torosa*. Phylogenetic and population genetic methods were integrated to infer history at deep and shallow time depths. Using a molecular clock, the subspecies *T. t. torosa* and *T. t. sierrae* were estimated to have diverged 7–13 Mya. Within *T. t. torosa,* genetically differentiated groups were identified along coastal California, in southern California, and in the southern Sierra Nevada. The coastal group exhibited isolation by distance, but a lack of genetic variation north of present-day Monterey was indicative of a recent range expansion. In southern California, a disjunct population in central San Diego County was genetically diverged from coastal populations to the north (Nei's genetic distance of 0.113). However, mtDNA and protein data were geographically discordant regarding the boundary between the coastal and southern Californian groups, and a biogeographical scenario was developed to account for this discordance. The southern Sierran clade of *T. t. torosa* was weakly diverged from coastal populations for mtDNA sequence variation, yet was strongly differentiated for allozyme variation (Nei's genetic distance of 0.17–0.20). Populations of *T. t. sierrae* exhibited substantial population structure, and showed a steeper pattern of isolation by distance than did coastal populations of *T. t. torosa*. These results are interpreted in consideration of the known geomorphological history of California.

ADDITIONAL KEYWORDS: allozymes – Bayesian analysis – biogeography – electrophoresis – haplotype network – isolation by distance – maximum likelihood – mismatch distribution – mitochondrial DNA.

INTRODUCTION

The history of species can be influenced profoundly by geomorphological evolution, such as mountain-building or the removal of barriers to dispersal. Such events affect patterns of genetic structure, and it is possible to infer the history of a lineage using molecular markers and to compare that history against known geological change (Avise, 2000; Brunsfeld *et al*., 2001; Jockusch & Wake, 2002). Multiple levels of divergence may be recoverable in the history of a lineage. For instance, vicariance events may be responsible for deep phylogeographical structure, such as reciprocally monophyletic lineages, while recent demographic episodes, such as range expansion or population bottlenecks, shape patterns of genetic diversity within and among populations (e.g. Kuchta & Meyer, 2001; Matocq, 2002; Carstens *et al*., 2004; Mahoney, 2004; Kuchta & Tan, 2005). Because of its geomorphological complexity, phylogeographical studies in western North America are particularly informative regarding the interaction of species diversification and landscape evolution (Yanev, 1980).

Here we present a phylogeographical study of the California newt, *Taricha torosa* (Rathke), using mtDNA sequences and allozyme variation. Two subspecies of *T. torosa* are currently recognized, the coast

*Corresponding author. Current address: University of California, Santa Cruz, Department of Ecology and Evolution, Earth & Marine Sciences, Room A316, Santa Cruz, CA 95064, USA. E-mail: skuchta@biology.ucsc.edu
†Current address: University of Manoa, Hawaiian Evolutionary Biology Program, Pacific Biomedical Research Program, 3050 Maile Way, Honolulu, HI 96822, USA.

range newt, *T. t. torosa,* and the Sierra newt, *T. t. sierrae* (Stebbins, 2003). The former is distributed throughout the coast ranges of California, from Mendocino to Los Angeles County, with disjunct populations in the Cayumaca mountains of central San Diego County. In addition, Tan & Wake (1995), using mtDNA sequence data, showed that populations in the southern Sierra Nevada, from Tulare to Kern County, are related more closely to *T. t. torosa* than they are to *T. t. sierrae* (Fig. 1). *Taricha t. sierrae* is distributed throughout the Sierra Nevada and southern Cascades, from Shasta County in the north to Tulare County in the south (Fig. 1). Note, however, that some sources continue to recognize populations in the southern Sierra Nevada as belonging to *T. t. sierrae* (e.g. Petranka, 1998; Stebbins, 2003). In this paper, using

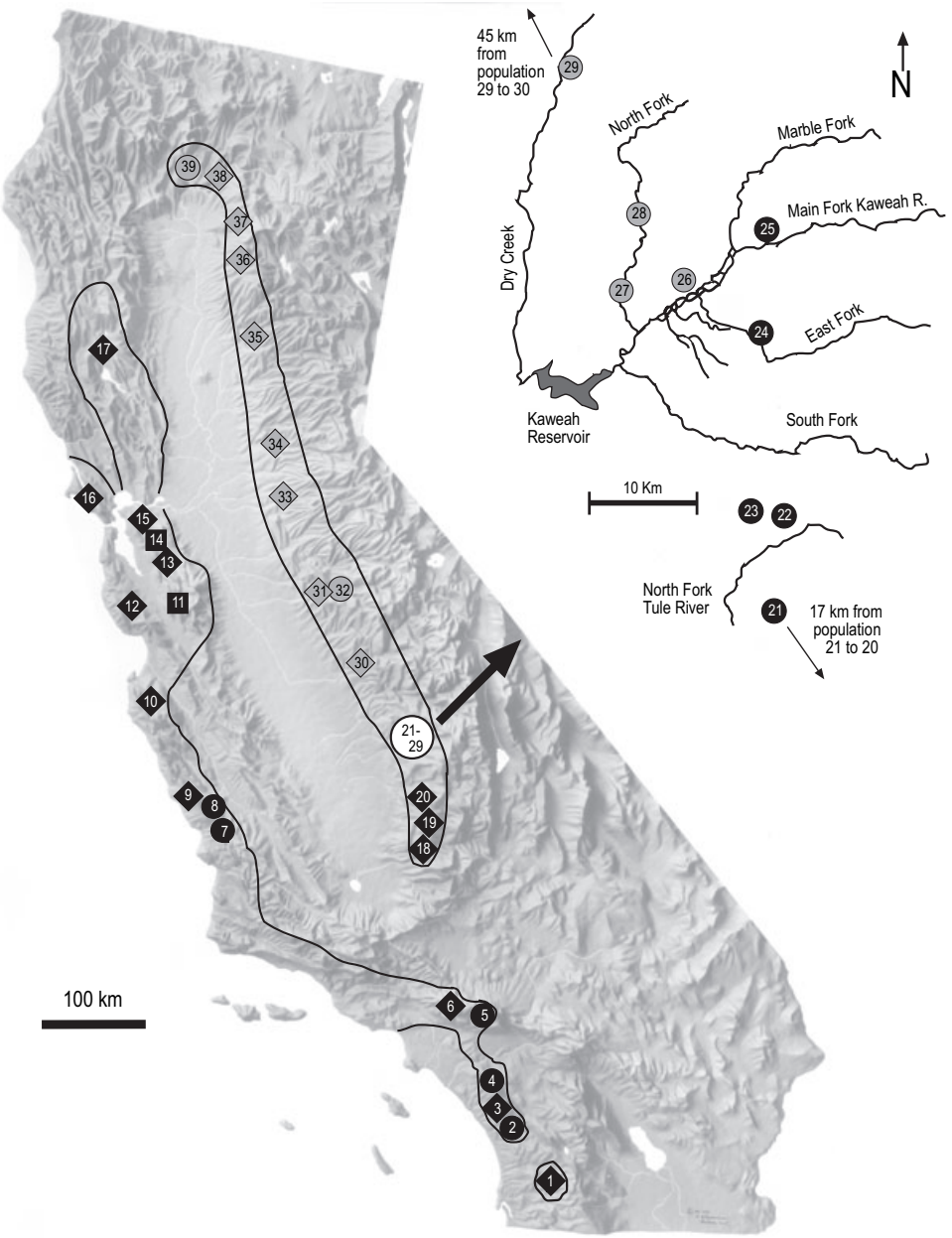

Figure 1. Map of California showing the collecting localities for *Taricha torosa*. Population numbers correspond to those in Table 1. Black symbols designate populations of *T. t. torosa,* and grey symbols designate populations of *T. t. sierrae*; symbol shapes identify the types of data collected for each population: allozymes (□), mtDNA cytochrome *b* sequence (○), or both (◇). The inset displays a region of denser sampling where *T. t. torosa* and *T. t. sierrae* contact.

improved mtDNA sampling and a detailed survey of allozyme variation, we test the hypothesis populations in the southern Sierra Nevada are most closely related to coastal populations of *T. t. torosa*.

Evolution of the Californian landscape

The formation of the coast ranges of central California is complex, and has influenced patterns of differentiation in many Californian species (Jockusch & Wake, 2001; Calsbeek, Thompson, & Richardson, 2003). Prior to the early Pleistocene, the present-day Central Valley was inundated with seawater (Yanev, 1980). Collision of the North American Plate with the Pacific Plate generated uplift, and by 5–3 Mya the coast ranges, which originated as islands, were fully integrated with the North American Plate. This created a large marine embayment in the present-day Central Valley that drained out through the Monterey Bay region (Dupré, 1990; Sims, 1993; Hall, 2002). Today, the Central Valley drainages exit via Carquinez Strait into San Francisco Bay, but this route is only 600 000 years old (Sarna-Wojcicki *et al*., 1985). The Monterey Bay region is consequently a major Californian biogeographical boundary, and many taxa show concordant phylogeographical breaks in this region (Wake, 1997; Calsbeek *et al.*, 2003).

The Sierra Nevada mountains are another major geological feature of biogeographical importance in California. The range is old, having existed since the late Cretaceous (House, Wernicke & Farley, 1998), though there was a second period of uplift *c*. 5 Mya (Wakabayashi & Sawyer, 2001). Recently, several phylogeographical studies have documented southern California and coast range lineages occupying the southern Sierra Nevada, to the exclusion of central Sierran lineages (summarized in Macey *et al*., 2001; Calsbeek *et al*., 2003). In this paper, we interpret patterns of genetic and phylogenetic differentiation in *T. torosa* in light of the known geological history of the Californian landscape.

MATERIAL AND METHODS

Protein electrophoresis: laboratory techniques and population sampling

Collections were made throughout the range of *T. torosa* (Table 1; Fig. 1). Specimens were sacrificed in 25% chlorotone, and heart, liver, and intestine were removed and frozen at –70 °C. Carcasses have been stored as vouchers in the Museum of Vertebrate Zoology (MVZ), University of California, Berkeley. Thirty-four enzymatic products encoded by 45 loci were surveyed (enzyme and buffer systems are provided in table 2 of Kuchta & Tan, 2005), and standard methods of starch gel electrophoresis were employed (Murphy *et al*., 1996; Tan, 1993). Twenty-three populations, totaling 198 individuals, were analysed (Table 1; Appendix). Fifteen of these populations were assignable to *T. t. torosa*, and eight to *T. t. sierrae* (Fig. 1). Four populations (34 individuals) of *T. rivularis* (Twitty) (Table 1) and 19 populations (109 individuals) of *T. granulosa* (Skilton) (Kuchta & Tan, 2005) were used as outgroups for phylogenetic analyses.

Cytochrome *b* sequence variation: laboratory techniques and population sampling

Tan & Wake (1995) presented data on 20 cytochrome *b* haplotypes (up to 375 bp) from 22 populations (36 individuals) of *T. torosa*. These data, which we refer to here as dataset #1, have been incorporated into this study. Haplotypes in dataset #1 were amplified using the primers MVZ15 and Cytb2, corresponding to nucleotide positions 19 to 405 of the cytochrome *b* gene (Tan & Wake, 1995). Sequencing was done on manual gels, and the protocol is described in detail in Tan & Wake (1995). For this study we sequenced the cytochrome *b* gene (up to 778 bp) from an additional 26 individuals from 18 populations; this data is referred to here as dataset #2. Two of the individuals in dataset #2 were also used by Tan & Wake (1995) in dataset #1; we replaced those in dataset #1 with the new sequences because the newer sequences are longer. For dataset #2, the primers MVZ15 and MVZ16 were used to amplify the region between nucleotide positions 19 and 804 of the cytochrome *b* gene (Moritz, Schneider & Wake, 1992). A 377 Automated Sequencer (Applied Biosystems, Inc.) was used and standard protocols were employed (details provided in Kuchta & Tan, 2005). The combined cytochrome *b* dataset included 60 haplotypes from 37 populations within *T. torosa* (Table 1). Three outgroup species were used in phylogenetic analyses, including two haplotypes of *Notophthalmus viridescens* (Rafinesque), 19 haplotypes (from 39 individuals) of *T. granulosa* (see Kuchta & Tan, 2005), and two haplotypes (from six individuals) from three populations of *T. rivularis*. Five of the latter sequences were obtained for this study; one was presented in Tan & Wake (1995). All sequences have been deposited in GenBank under accession numbers DQ196241–DQ196308.

Phylogenetic analysis

For phylogenetic analyses, all available protein and mtDNA data for all species of *Taricha* were used (Table 1), including data on *T. granulosa* presented in

Table 1. Locality information for *Taricha torosa* and *T. rivularis*, with population numbers corresponding to Figure 1

Pop.	County	Specific locality	Latitude/Longitude	Sample size		Specimen identification no.
				Allo.	mtDNA	
Taricha torosa						
1	San Diego	Cedar Creek, Cleveland National Forest	32.3200 N/116.7333 W	4	1, 1‡	MVZ[1] 219826†, -27*, -28*, -29†
		Boulder Creek, Cleveland National Forest	32.9634 N/116.6637 W	1	1	MVZ 219825*
2	San Diego	Camp Pendelton, Roblar Dr, 500 m upstream from jct. with Deluz Creek	33.3750 N/117.3500 W	–	1‡	MVZ 223143
3	Orange	Trabuco Canyon, Santa Anna mountains, Cleveland National Forest	33.6827 N/117.5029 W	8	2	MVZ 219817*, -18* to -24†
4	Riverside	Upper Tanaja Canyon, Cleveland National Forest	33.5272 N/117.3742 W	–	1‡	MVZ 223141
5	Los Angeles	San Dimas Creek, Angeles National Forest	34. 1833 N/117.8167 W	–	1‡	MVZ 223138
6	Los Angeles	Clear Creek, San Gabriel Mountains, Angeles National Forest	34.2715 N/118.1531 W	3	2	MVZ 219814*, -15*, -16†
7	San Luis Obispo	Tassajara Creek, West of Santa Margarita, Cleveland National Forest	35.3834 N/120.6705 W	–	1‡	MVZ 236243
8	San Luis Obispo	Santa Rita, Old Creek Road, 3.6 miles SW of Vineyard Road at Templeton	35.5231 N/120.6708 W	–	1‡	MVZ 236242
9	San Luis Obispo	San Simeon Creek, near Hwy 1, inland of San Simeon State Beach	35.6075 N/121.0896 W	8	2	MVZ 213093†, -94*, -95†, -96* to -100†
10	Monterey	Hastings Natural History Reserve, Carmel Valley	36.3853 N/121.5543 W	3	1	MVZ 217912† to -14*
11	Santa Clara	San Antonio Road, San Antonio Valley, East of Santa Clara Valley	37.3559 N/121.5662 W	7	–	MVZ 158856† to -62†
12	San Mateo	Bear Gulch Creek, near Woodside, Santa Cruz mountains	37.4268 N/122.2529 W	10	2	MVZ 217877†, -78*, -79†, -80†, -81* to -86†
13	Alameda	Pleasanton Annex Site, hills between Pleasanton and Hayward	37.6553 N/121.9862 W	10	1	MVZ 217917†, -18* to -26†
14	Contra Costa	Los Trampas Creek, west of Las Trampas Peak, near Moraga	37.8291 N/122.0717 W	5	–	MVZ 217898† to -902†
15	Contra Costa	Bear Creek Road, near Briones Regional Park	37.9324 N/122.1352 W	10	2	MVZ 217871, -72 MVZ 217861† to -70†,
16	Marin	Point Reyes National Seashore	37.9566 N/122.7792 W	10	1	MVZ 216136†, -37†, -38* to -42† MVZ 217927† to -29†
17	Lake	Old State Hwy, 0.1 miles N. Hwy 20	39. 1862 N/123.0255 W	5	1	S10757† to -59†[2]; S10761†, -62*

18	Kern	Mill Creek, Sequoia National Forest, SW of Isabella Reservoir	35.5426 N/118.6170 W	6	2	MVZ 219098*, -99* to -103†
19	Tulare	Deer Creek, Hot Springs Road, Sequoia National Forest	35.8846 N/118.6568 W	3	1	MVZ 219846* to -48†
20	Tulare	Camp Nelson, near S. Fork Tule River, Sequoia National Forest	36.1393 N/118.6126 W	7	2	MVZ 219849*, -50* to -55†
21	Tulare	Rancheria Creek, off Forest Road 220, Sequoia National Forest	36.2167 N/118.7667 W	–	2‡	MVZ 223147, -48
22	Tulare	Jenny Creek, entering North Fork Tule River, Sequoia National Forest.	36.2750 N/118.7333 W	–	1‡	MVZ 223146
23	Tulare	Kramer Creek, at jct. with Backbone Road, Sequoia National Forest	36.2989 N/118.7908 W	–	2‡	MVZ 223149, -50
24	Tulare	Grunigan Creek, near jct. with Mineral King Road	36.4422 N/118.7703 W	–	3‡	MVZ 237869 to -71
25	Tulare	Hospital Creek, ~1 mile N. of Hospital Rock, Sequoia National Park	36.5264 N/118.7719 W	–	1‡	MVZ 237882
26	Tulare	Sycamore Creek, along Sheppard Saddle Road, Sequoia National Park	36.4949 N/118.8503 W	–	3‡	MVZ 223152, -53; MVZ 237956
27	Tulare	North Fork Road, 4.4 miles N. of Hwy 198	36.4914 N/118.9178 W	–	1‡	MVZ 237905
28	Tulare	Yucca Creek, end of North Fork Road, Sequoia National Park	36.5461 N/118.8969 W	–	1‡	MVZ 237931
29	Tulare	Near Eshom Creek Campground & Dry Creek, Sequoia National Forest	36.6705 N/118.9719 W 36.7042 N/118.9574 W	– –	2 ‡ 1‡	MVZ 237814, -16 MVZ 223151
30	Fresno	Junction of Jose Basin Road and Jose Basin, E. of Shaver Lake, Sierra National Forest	37.1298 N/119.3756 W	10	2	MVZ 197468† to -74*, -75* to -77†
31	Mariposa	Sherlock Creek, Merced River Drainage, near McClure Reservoir	37.5806 N/120.0762 W	10	2	MVZ 175401† to -04*, -05* to -10†
32	Mariposa	Slope above Hwy 140, near South fork of the Merced River	37.6544 N/119.8949 W	–	1‡	MVZ 237707
33	Calaveras	3.2 miles West of West Point, North of Middle Fork of Mokelumne River	38.3870 N/120.5671 W	9	2	MVZ 185816†, -17† MVZ 185872† to -74† MVZ 197463, -64
34	El Dorado	Vicinity of the American River and Placerville	38.7600 N/120.8182 W	5	2	MVZ 197461*, -62* MVZ 202301† to -03†
35	Butte	Cherokee Creek, West side of Oroville Reservoir	39.5803 N/121.5510 W	10	2	MVZ 219081† to -90† MVZ 219091, -92

Table 1. *Continued*

Pop.	County	Specific locality	Latitude/Longitude	Sample size		Specimen identification no.
				Allo.	mtDNA	
36	Tehema	South Fork Battle Creek, SW of Manton, Sacramento River Drainage	40.3333 N/121.8333 W	6	–	MVZ 217903† to -08†
		Paynes Creek, south of Battle Creek, Sacramento River Drainage	40.3416 N/121.8553 W	1	1	MVZ 217911*
37	Shasta	North Fork Bear Creek, North of Shingletown, SE of Shasta Reservoir	40.5613 N/121.8978 W	3	1, 1‡	MVZ 172748*, -49* MVZ 173373†
38	Shasta	Squaw Creek, North of Squaw Creek Arm of Shasta Reservoir	40.8551 N/122.1201 W	10	1	MVZ 219831* to -40†
39	Shasta	0.3 miles from Mt. Gate Limestone Quarry sign (and jct with Radcliff Road), on Fawndale Road	40.9239 N/122.4331 W	–	1‡	MVZ 237593
Taricha rivularis						
40	Sonoma	Stewart Point Skaggs Springs Road, 10.1–22.6 miles East of Stewards Point;	38.6761 N/123. 2000 W	10	–	MVZ 217829* to -38*
		Skaggs Springs	38.6931 N/123.0256 W	4	–	MVZ 161863† to -66†
41	Sonoma	Big Sulphur Creek, 13–13.7 miles East U.S. Hwy. 101 on Geysers Road	38.8043 N/122.8355 W	9	2	MVZ 217842† to -50† MVZ 217851, -52
42	Mendocino	14.1 miles East of Flynn Creek Road on Orr Springs Road	39.2429 N/123.4069 W	3	2	MVZ 158853*, -54*, -55†
43	Humboldt	Eubank Creek Drainage, ~3 miles South of Ettersburg	40.1070 N/123.9534 W	8	2	MVZ 219803† to -10† MVZ 219811, -12
Notophthalmus viridescens						
44	Brunswick	Temporary Lake 2 miles NW of Southport (North Carolina)	33.9736 N/78.0614 W	–	1	MVZ 161852†
45	Alachua	River Styx Crossing, Hwy. 346 (Florida)	29.5169 N/82.2219 W	–	1‡	MVZ 205719†

*Specimens for which we have mtDNA sequence data and electrophoretic data. †Specimens for which we have electrophoretic data only. Specimen identification numbers with no symbol are those for which we had mtDNA sequence data only.
The mtDNA sample sizes have no symbols for dataset #1 and are designated ‡ for sequences added by dataset #2 (see Materials and Methods).
[1]Museum of Vertebrate Zoology, University of California, Berkeley, California. [2]Salamander Frozen Tissue Collection, Museum of Vertebrate Zoology, University of California, Berkeley, California.
Allo., allozymes; Pop., population.

Kuchta & Tan (2005). This was because increased phylogenetic accuracy may result from improved taxon sampling (Poe, 1998).

Allozymes

Parsimony with step matrices was used to construct a phylogenetic hypothesis from the protein data (Mabee & Humphries, 1993). Loci were scored as characters, and allelic combinations as character states (Mickevich & Mitter, 1981). The gain or loss of an allozyme was scored as a single step, and thus ordered. For example, to go from character state '*ab*' to state '*ac*' is two steps, one for the loss of allozyme '*b*' and one for the gain of allozyme '*c*'. A complete step matrix was used to allow hypothetical common ancestors to possess character states not present in the operational taxonomic units (OTUs) if it was most parsimonious to do so (Mabee & Humphries, 1993). The logic is that in going from one character state (for example, '*ab*') to another ('*cd*'), it may be necessary to pass through character states not present in the OTUs ('*bc*'). This approach to parsimony performs well on real datasets (Wiens, 2000).

The shortest trees were estimated with PAUP* 4.0b10 (Swofford, 2002). A heuristic search option with ten random addition replicates was employed with the tree bisection–reconnection (TBR) branch-swapping algorithm. The outgroup was designated as *T. rivularis* (Larson, Weisrock & Kozak, 2003). Bootstrapping (Felsenstein, 1985) and decay indices (Bremer, 1994) were used to estimate levels of clade support.

Cytochrome b

To test for mutational saturation in the dataset, the absolute numbers of transitions and transversions at each codon position (1st, 2nd, and 3rd) were plotted against maximum likelihood (ML) distances (parameters chosen with Modeltest 3.06; Posada & Crandall, 1998). The number of mutational differences is expected to increase linearly as a function of genetic distance when the data are unsaturated; mutational saturation is detected when greater genetic distances are not reflected in a greater number of mutational differences.

For ML analyses, the model that best fitted the cytochrome *b* data was determined using a hierarchical likelihood ratio test, as implemented in the program Modeltest 3.06 (Posada & Crandall, 1998). The model chosen was Hasagawa, Kishino & Yano (1985)'s (denoted HKY), including a parameter for substitution rate heterogeneity among sites ($\Gamma = 0.2160$). Nucleotide frequencies under this model were estimated as: A = 0.3083; C = 0.3049; G = 0.1355; T = 0.2516. The transition/transversion ratio was estimated as 7.4275. All sites were assumed to be variable. The ML analysis employed a heuristic search routine, TBR branch swapping, and a starting tree estimated by neighbour-joining.

Bayesian phylogenetic analyses were conducted with MrBayes 2.01 (Huelsenbeck & Ronquist, 2001). The program MrModeltest 1.1 (Nylander, 2002) was used to estimate the simplest evolutionary model which fitted the data. The HKY (Hasagawa *et al*., 1985) model was chosen, including a gamma parameter. The analysis was initiated with random starting trees, and carried out for 2.0×10^6 generations. The Markov chains were sampled every 100 generations, for a total of 20 000 sample points. After excluding 'burn in' generations, a majority rule consensus tree was constructed. The percentage of times that a particular clade is recovered is its posterior probability (Larget & Simon, 1999; Lewis, 2001).

To verify that the posterior probability values had not become 'stuck' on a local optimum, Bayesian analyses were repeated five times with different random starting trees. The log-likelihood values were compared to see that they had converged, and the posterior probabilities of the clades were compared for general congruence. In all runs, Metropolis-coupled Markov chain Monte Carlo methods (four 'heated chains') were used to improve the ability of the Markov chains to find alternate optima.

Regional diversity: allozyme variation

Multidimensional scaling

Multidimensional scaling (MDS) was used to graphically depict the genetic similarity among populations. MDS is a class of ordination techniques that displays the complex relationships among populations in a small number of dimensions (Lessa, 1990). The advantage of MDS is that it allows visualization of population similarity without imposing a hierarchical structure on the data, which may be an inappropriate assumption when dealing with intraspecific differentiation (Felsenstein, 1982; Lessa, 1990). When interpopulational variation is a function of distance alone, MDS predicts that the first two dimensions will produce clustering patterns similar to a geographical map of the populations (Jackman & Wake, 1994; Tilley & Mahoney, 1996; Kuchta & Tan, 2005). Note that genetically similar clusters do not necessarily identify historical relationships (clades) (de Queiroz & Good, 1997).

MDS was performed using the program Statistica (StatSoft, Inc.). Data were input as a matrix of Nei's (1978) genetic distances (D_N), but Rogers's (1972) distances provided equivalent results (data not shown). Scree plots were used to determine the number of

dimensions required to sufficiently accommodate the observed variation.

Isolation by distance

The accumulation of genetic differentiation among populations with increased geographical spread as a result of restricted dispersal relative to the geographical range was first explored by Wright (1943), who termed the phenomenon 'isolation by distance' (IBD). IBD in this study was examined by plotting Nei's (1978) unbiased D_N among pairwise population comparisons against geographical distance (see also Good & Wake, 1992; Jackman & Wake, 1994; Tilley & Mahoney, 1996; de Queiroz & Good, 1997; Kuchta & Tan, 2005). Analyses using the method of Slatkin (1993) provided equivalent results (data not shown; see Kuchta, 2002). Mantel tests (100 000 randomizations), which correct for the nonindependence among pairwise comparisons present in IBD plots, were used to test for a significant correlation between geographical and genetic distances (IBD). For regions showing significant IBD, reduced major axis (RMA) regression was used to calculate the slope, *y*-intercept, and coefficient of determination (r^2). The 99% confidence intervals for slope estimates were measured by jack-knifing over populations (1000 randomizations). Based on simulation data, Hellberg (1994) has shown that RMA regression is superior to ordinary least squares regression for this purpose. The computer program IBD (Bohonak, 2002) was used to calculate Mantel tests and RMA regression statistics.

One can also analyse the genetic relationships between regions (or clades). If two regions form a collection of demographically connected populations, a regression on inter-region comparisons will intersect the origin. In contrast, if there has been a restriction of gene flow between the regions, the regression will intersect above the origin (see also Good & Wake, 1992; de Queiroz & Good, 1997). For comparisons of IBD between regions (which lacked within-region comparisons), Mantel tests could not be calculated, and the program RMA 1.16 (Bohonak, 2004) was used to find the best-fit line. However, because of the non-independence among datapoints, between-region regressions are presented here as a visual aid only, and should be interpreted with caution.

REGIONAL DIVERSITY: CYTOCHROME *B*

Diversity indices

Genetic diversity indices were used to compare patterns of genetic diversity among lineages. Diversity indices were calculated: (1) for *T. torosa*, including both subspecies; (2) separately for the subspecies *T. t. torosa* and *T. t. sierrae*; (3) for three mtDNA clades within *T. t. torosa* (the coastal, southern Californian, and southern Sierran clades). Computed diversity indices included: (i) haplotype diversity, h, the probability that two randomly selected haplotypes were different from each other; (ii) nucleotide diversity, π, the average number of nucleotide differences per site between two sequences; (iii) sequence diversity, κ, the average number of nucleotide differences between paired sequences (Nei, 1987). DNAsp 4.0 (Rozas *et al*., 2003) was used for all calculations.

Haplotype networks

Haplotype networks, which depict population-level genealogical relationships, are useful at low levels of divergence when gene trees may not be bifurcating, and thus the hypothesis of a hierarchical relationship among haplotypes is violated. Haplotype networks using statistical parsimony were generated with TCS 1.13 (Clement, Posada & Crandall, 2000).

Mismatch distributions

Histograms of the number of pairwise mutational differences among haplotypes, or 'mismatch distributions', were used to distinguish population differentiation from range expansion. Under a model of recent population expansion, a mismatch distribution will resemble a Poisson distribution (Slatkin & Hudson, 1991). Conversely, with population differentiation, a mismatch distribution becomes multimodal. We generated mismatch distributions for populations from a number of geographical regions, and compared these distributions to the distribution expected under a step-wise expansion model (Schneider & Excoffier, 1999); significance was assessed via parametric bootstrapping of the dataset (10 000 replicates). All analyses were done with Arlequin 2.001 (Schneider, Roessli & Excoffier, 2000).

Molecular clock estimation

Tan & Wake (1995) estimated the rate of cytochrome *b* sequence divergence in *Taricha* by calibrating with North American salamandrid fossils . Their estimate was 0.8% divergence per Myr. We employed this clock to estimate the timing of biogeographical events within *T. torosa.* Genetic distances within and among clades of *T. torosa* were estimated using both uncorrected sequence divergence and ML estimates of divergence. Estimates of divergence were corrected for ancestral polymorphism using the equation $D_{xy} = D - 0.5(D_x - D_y)$, where D_x and D_y designate average divergence within different clades and D is the total average divergence between clades (Avise & Walker, 1998; Matocq, 2002). The method factors out retained ancestral polymorphism in estimating divergence among clades, assuming that historic levels of diversity are similar to present-day levels. This may be an inappropriate assumption for various reasons (e.g. the

coastal clade of *T. torosa* appears to have undergone a diversity-reducing range expansion in the past), but it remains a simple, reasonable method for accounting for ancestral variation. Because of the difficulties of using molecular clocks to estimate the time since divergence (Hillis, Moritz & Mable, 1996), age estimates in this paper should be interpreted with caution.

RESULTS

Phylogenetic analysis: allozyme variation

Parsimony

In the allozyme dataset, 30 loci were phylogenetically informative, three variable loci were uninformative for parsimony, and 12 loci were monomorphic. A maximum of five allozymes was found at any one locus. A parsimony analysis resulted in 1318 most parsimonious trees, each 243 steps long. Figure 2 is a strict consensus of these trees. The consistency index was 0.502 (rescaled CI = 0.418), and the retention index (RI) was 0.834.

T. rivularis and *T. granulosa* both formed monophyletic clades. The clade representing *T. rivularis* was supported strongly, with bootstrap support of 100% (decay index (DI) = 15 steps); *T. granulosa* had a bootstrap support of 91% (DI = 8). The monophyly of *T. torosa* was also monophyletic, though this is not statistically supported (bootstrap support < 50%; DI = 1). In addition, there was limited support for phylogenetic structure within *T. torosa*. Nonetheless, the results are reasonable on geographical grounds, and the tree is congruent in many respects with the mtDNA phylogeny and other analyses (results described below). In *T. torosa*, the disjunct southern Californian population (population 1) was sister to a clade consisting of all the coast range populations (populations 3–17). A southern Sierran clade (populations 18–20) was supported strongly (bootstrap support = 95%; DI = 4), and this clade was sister to the southern Californian + coastal clade (populations 1–17). Together, these three clades constituted *T. t. torosa*, which was sister to *T. t. sierrae* (30–38). Within *T. t. sierrae*, the northern Sierra Nevadan populations,

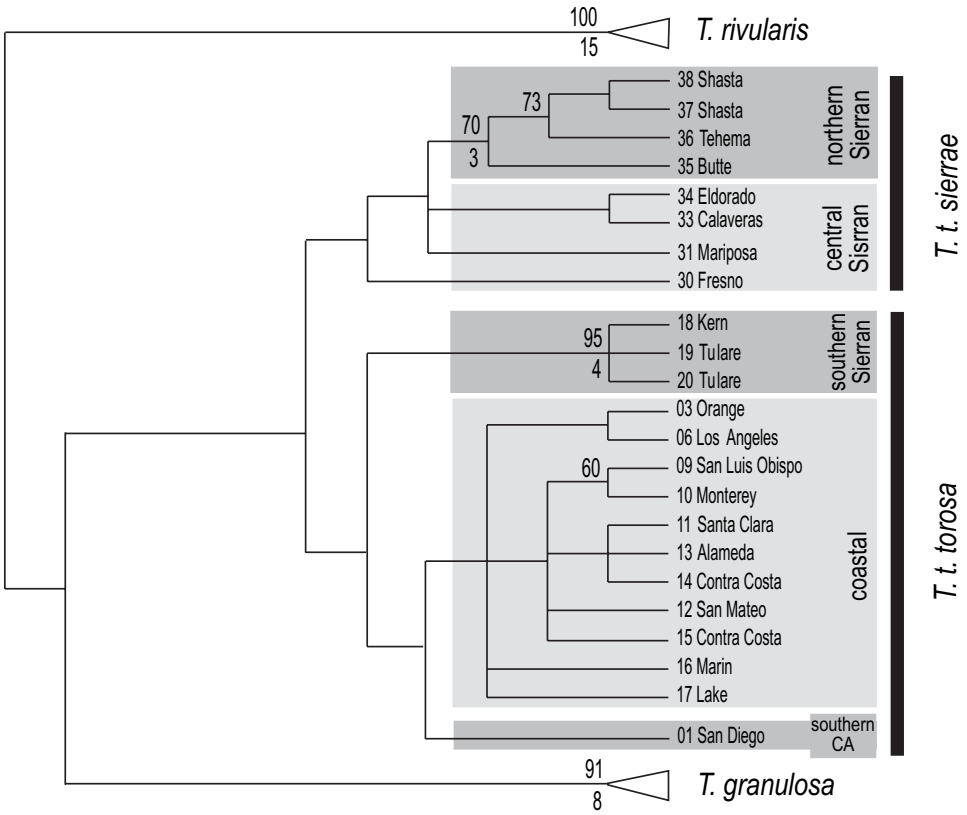

Figure 2. Results of a parsimony analysis of the allozyme data. Numbers above nodes are bootstrap values (500 replicates) above 60%; numbers below nodes are decay indices. The tips of the branches are labelled with population numbers (Table 1; Fig. 1) and county. Shading identifies groupings discussed in the text.

from Butte to Shasta County (populations 35–38) were monophyletic (bootstrap support = 70%; DI = 3), but the central Sierra Nevadan populations (populations 30–34) were paraphyletic. Within *T. t. sierrae*, there was a nested, stepwise relationship among the populations from south to north.

Phylogenetic analysis: cytochrome *b*

Saturation curves

When ML distances were plotted against the absolute number of pairwise differences in transversions and transitions, some mutational saturation was detected (data not shown; see Kuchta, 2002). First and second position transitions had minor saturation, but higher levels of saturation were found for third position transitions, especially within dataset #1, and between ingroup and outgroup taxa. There was no saturation in first and second position transversions, but minor saturation at the third position between ingroup and outgroup taxa was detected.

Maximum likelihood and Bayesian analyses

Five Bayesian runs with separate random starting trees converged on similar log-likelihood values after about 200 generations. To be conservative, the first 500 generations were excluded as 'burn in' from all runs, leaving 19 500 trees. Majority rule consensus trees were constructed for each run, and all five runs had identical topologies. Thus, the posterior probability values likely did not become stuck on local optima.

The ML and Bayesian analyses resulted in very similar trees, and are discussed together here (Fig. 3).

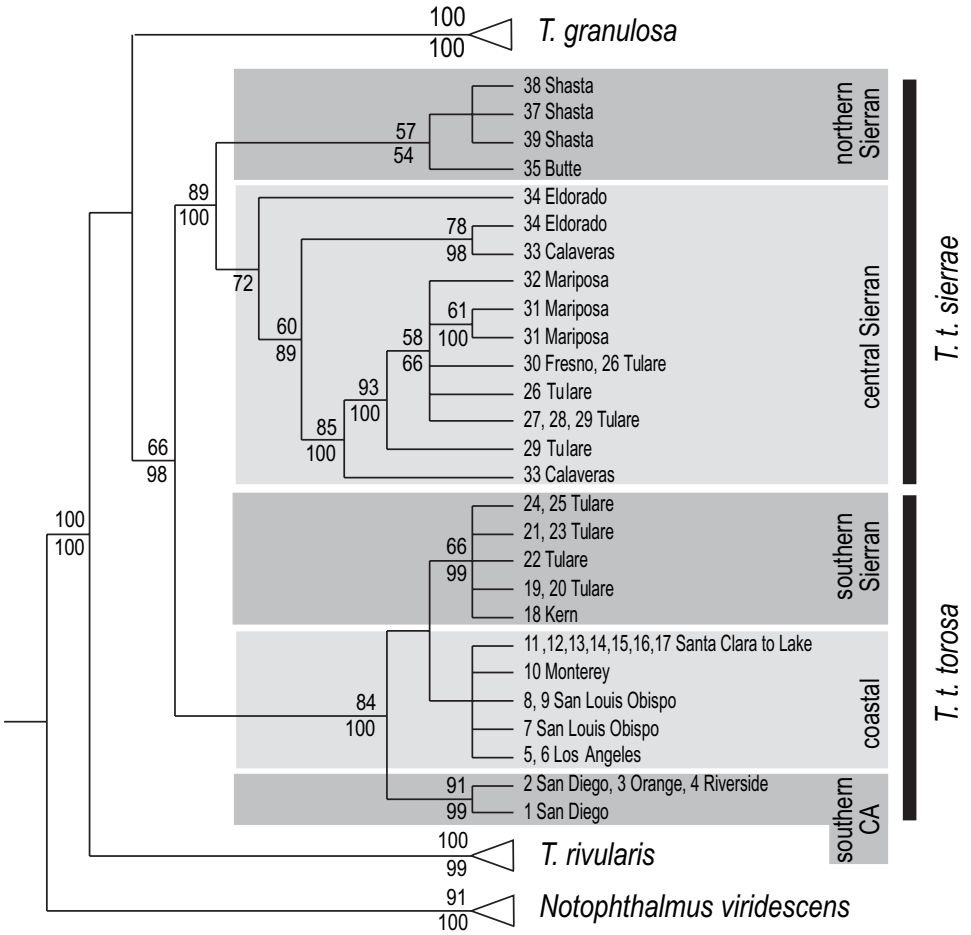

Figure 3. Strict consensus of the five shortest trees from a maximum likelihood analysis. Bayesian analysis yielded nearly identical results. Numbers above nodes are bootstrap support values > 50% from 100 replicates; numbers below nodes are Bayesian support values > 50% from a majority rule consensus of 19 500 trees. Tips of branches are labelled with population numbers (Table 1; Fig. 1) and county. Shading identifies clades discussed in the text.

In both Bayesian and ML analyses, *T. rivularis* was monophyletic (bootstrap support = 91%; posterior probability = 100%), and was sister to a *T. torosa* + *T. granulosa* clade. However, this latter clade lacked statistical support. The monophyly of *T. torosa* had moderate support (bootstrap support = 66%; pp = 98%), but the two described subspecies were recovered with stronger support (*T. t. torosa*: bootstrap support = 84%, pp = 100%; *T. t. sierrae*: bootstrap support = 89%, pp = 100%). Within *T. t. torosa*, the southern Sierran clade (bootstrap support = 66%; pp = 99%) was sister to a poorly supported, unresolved coastal clade (bootstrap support and pp < 50%). The southern Californian clade (populations 1–4; bootstrap support = 91%; pp = 99%) was sister to the coastal + southern Sierran clade. The major feature distinguishing the Bayesian and ML trees was that in the former (data not shown) coastal clade populations formed an unresolved polytomy that included the southern Sierran clade. Within *T. t. sierrae,* there were two monophyletic clades corresponding to the northern Sierra Nevadan (populations 35–38: bootstrap support = 57%; pp = 54%) and central Sierra Nevadan (populations 30–34: bootstrap support < 50%; pp = 72%) regions. Within the central Sierra Nevada, two haplotypes from Calaveras County (population 33) were located in different regions of the tree, one grouping with Eldorado County (population 34) to the north (bootstrap support = 78%; pp = 98%) and the other with populations to the south (bootstrap support = 85%; pp = 100%); in addition, the two sequences from the Eldorado County population were distantly related. Populations at the southern end of the central Sierra Nevadan clade (from Mariposa and Tulare Counties; 26–32) formed a strongly supported lineage (bootstrap support = 93%; pp = 100%).

Two important features differed between the trees generated by the allozyme and cytochrome *b* datasets (Figs 2 and 3). First, the allozyme tree postulated the southern Sierran clade as sister to the coastal + southern Californian clade, whereas the cytochrome *b* phylogenies portrayed the southern Sierran clade as most closely related to the coastal clade. Second, the location of the geographical border between the coastal clade and the southern Californian clade was discordant between the two data types. In the allozyme data, the southern Californian region was composed of a single, disjunctly distributed population in San Diego County (population 1), while the coastal clade contained populations 3–17. In contrast, in the cytochrome *b* data, populations from San Diego (populations 1 and 2), Orange (population 3), and Riverside (population 4) Counties formed the southern Californian clade, while populations 5–17 composed the coastal clade.

Regional diversity: allozyme variation

Multidimensional scaling

Table 2 displays the matrix of Nei's (1978) D_N and Rogers's (1972) genetic distances among population samples. The allozyme frequencies within populations are provided in the Appendix. A scree plot suggested two dimensions to be adequate to summarize the observed variation (data not shown; see Kuchta, 2002). The MDS analysis of *T. torosa* (Fig. 4) identified three clusters of populations, including the coastal cluster (populations 3–17), the southern Sierra Nevadan cluster (populations 18–20), and the central and northern Sierra Nevadan clusters (i.e. *T. t. sierrae*; 30–38). The single population in southern California (population 1) was distinct from these clusters. These clusters (and population 1) corresponded to the lineages identified in the parsimony analysis of the allozyme data (but differed from the mtDNA tree in some respects). Visually, the MDS analysis roughly resembled a plot of the populations of *T. torosa* on a map (compare Fig. 4 with Fig. 1). However, irregularities existed with respect to geographical relations. For example, the coastal and southern Sierran clusters were plotted as tighter groupings of populations than their geographical positions would predict. Additionally, in the coastal cluster, populations geographically closest to the southern Californian population were plotted the furthest away (populations 1 vs. 3, 6, and 9; Fig. 4). In contrast to the coastal populations, the central and northern Sierran clusters (*T. t. sierrae*) were broad and organized loosely. In the central Sierra Nevada, populations 30 and 31 were distinctive in the second dimension, with populations 33 and 34 positioned between them. The northern Sierran cluster had higher values in the first dimension than did the central Sierran cluster, and was inverted relative to geography, with southern populations possessing higher values in the second dimension than did northern populations.

Patterns of allozyme differentiation among multidimensional scaling clusters

Because our sample sizes were moderate (range, 3–10 individuals), we could not compare with a high degree of confidence allele frequency differences among populations (Rannala, 1995; Wiens & Servedio, 2000). However, there were a number of patterns that made biogeographical sense and were concordant with other analyses (such as phylogenetic reconstructions), and below we present the most pertinent results; these should be interpreted with a degree of caution.

Within *T. torosa,* most MDS clusters (Fig. 4) possessed allozymes unique to that cluster and present in all populations of that cluster. Within *T. torosa,* the coastal cluster had such a pattern at two loci

Table 2. Nei's (1978; below diagonal) and Rogers's (1972; above diagonal) genetic distances between population pairs. Population numbers correspond to Fig. 1, Table 1, and the Appendix. The shading highlights comparisons within subspecies; unshaded regions are comparisons between species. The lines demarcate groupings discussed in the text

	Taricha torosa torosa															*Taricha torosa sierrae*							
Pop:	1	3	6	9	10	11	12	13	14	15	16	17	18	19	20	30	31	33	34	35	36	37	38
1	–	0.325	0.352	0.342	0.319	0.341	0.317	0.332	0.341	0.335	0.321	0.307	0.396	0.396	0.397	0.432	0.459	0.423	0.43	0.482	0.456	0.44	0.413
3	0.113	–	0.063	0.103	0.125	0.175	0.166	0.158	0.173	0.168	0.155	0.144	0.427	0.427	0.427	0.461	0.438	0.399	0.407	0.457	0.434	0.441	0.452
6	0.132	0.001	–	0.088	0.119	0.158	0.177	0.141	0.157	0.156	0.151	0.154	0.42	0.42	0.421	0.455	0.432	0.392	0.4	0.452	0.431	0.455	0.456
9	0.125	0.009	0.005	–	0.103	0.155	0.17	0.14	0.154	0.151	0.161	0.161	0.418	0.418	0.419	0.45	0.427	0.39	0.398	0.449	0.423	0.444	0.449
10	0.105	0.01	0.008	0.005	–	0.125	0.135	0.114	0.125	0.123	0.135	0.133	0.398	0.398	0.399	0.43	0.415	0.379	0.387	0.442	0.416	0.433	0.432
11	0.124	0.03	0.024	0.023	0.011	–	0.082	0.047	0.004	0.019	0.088	0.103	0.4	0.4	0.4	0.43	0.406	0.37	0.378	0.444	0.425	0.45	0.453
12	0.107	0.027	0.03	0.028	0.014	0.006	–	0.094	0.082	0.068	0.089	0.067	0.407	0.407	0.408	0.437	0.414	0.378	0.386	0.451	0.43	0.429	0.447
13	0.118	0.024	0.018	0.019	0.008	0.001	0.008	–	0.046	0.049	0.083	0.091	0.4	0.4	0.401	0.432	0.408	0.371	0.379	0.44	0.416	0.44	0.443
14	0.124	0.029	0.023	0.023	0.011	0	0.006	0.001	–	0.018	0.085	0.1	0.399	0.399	0.399	0.43	0.406	0.369	0.377	0.444	0.425	0.449	0.453
15	0.12	0.028	0.023	0.022	0.01	0	0.004	0.001	0	–	0.079	0.09	0.399	0.399	0.4	0.429	0.405	0.37	0.378	0.444	0.425	0.445	0.451
16	0.11	0.023	0.021	0.025	0.013	0.006	0.006	0.005	0.006	0.005	–	0.061	0.396	0.396	0.397	0.431	0.406	0.36	0.372	0.435	0.422	0.435	0.443
17	0.099	0.019	0.022	0.025	0.012	0.009	0.003	0.007	0.009	0.007	0.002	–	0.403	0.402	0.403	0.439	0.414	0.373	0.381	0.444	0.425	0.426	0.441
18	0.172	0.204	0.195	0.195	0.172	0.175	0.183	0.176	0.174	0.175	0.174	0.178	–	0.012	0.025	0.368	0.407	0.373	0.367	0.41	0.401	0.427	0.373
19	0.171	0.203	0.194	0.195	0.172	0.175	0.183	0.176	0.174	0.175	0.174	0.177	0	–	0.021	0.368	0.407	0.373	0.367	0.414	0.401	0.427	0.373
20	0.172	0.204	0.195	0.196	0.173	0.175	0.184	0.177	0.175	0.176	0.174	0.178	0	0	–	0.368	0.407	0.373	0.367	0.411	0.402	0.427	0.374
30	0.211	0.247	0.237	0.233	0.208	0.208	0.218	0.211	0.208	0.208	0.213	0.219	0.147	0.147	0.148	–	0.193	0.3	0.293	0.38	0.341	0.371	0.314
31	0.241	0.219	0.209	0.206	0.192	0.183	0.192	0.186	0.183	0.183	0.185	0.192	0.183	0.183	0.184	0.037	–	0.265	0.276	0.363	0.33	0.36	0.367
33	0.202	0.179	0.17	0.17	0.157	0.15	0.159	0.151	0.149	0.151	0.143	0.153	0.152	0.152	0.153	0.097	0.074	–	0.124	0.312	0.302	0.335	0.338
34	0.207	0.184	0.175	0.176	0.162	0.156	0.164	0.157	0.155	0.156	0.152	0.158	0.145	0.145	0.145	0.09	0.079	0.013	–	0.297	0.287	0.321	0.324
35	0.268	0.241	0.231	0.232	0.221	0.223	0.233	0.219	0.222	0.224	0.216	0.223	0.186	0.19	0.187	0.159	0.144	0.104	0.093	–	0.217	0.261	0.264
36	0.237	0.214	0.208	0.202	0.192	0.203	0.209	0.193	0.202	0.203	0.202	0.202	0.178	0.177	0.178	0.126	0.117	0.097	0.086	0.048	–	0.136	0.165
37	0.216	0.22	0.233	0.224	0.209	0.227	0.206	0.218	0.227	0.223	0.214	0.202	0.202	0.201	0.202	0.149	0.14	0.12	0.108	0.07	0.016	–	0.169
38	0.19	0.236	0.238	0.232	0.211	0.234	0.228	0.224	0.234	0.233	0.226	0.221	0.152	0.152	0.152	0.106	0.148	0.124	0.112	0.073	0.027	0.027	–

Population numbers correspond to those in Figure 1, Table 1, and the Appendix.

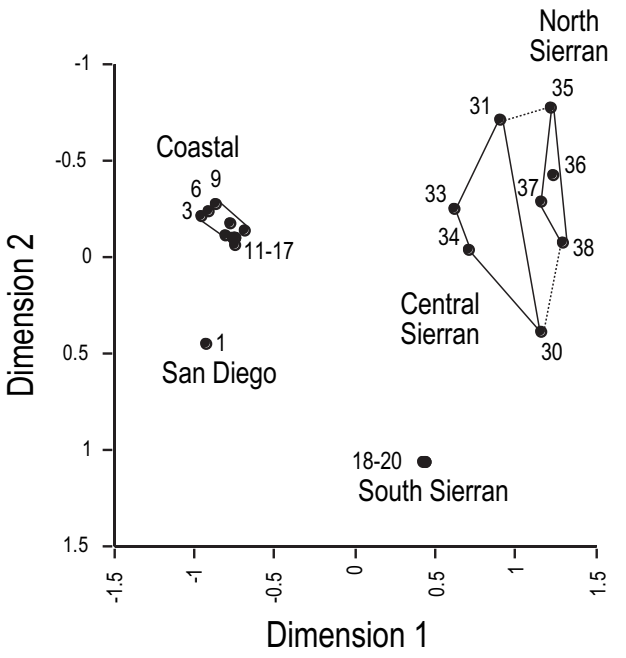

Figure 4. Multidimensional scaling of Nei's (1978) genetic distances among populations of *Taricha torosa*. Population numbers correspond to Table 1, Figure 1, and the Appendix.

(*GDAb*, *LA1a*; Appendix), the southern Sierran cluster at three loci (*AAT1b*, *EST2d*, *CAH2c*), and the central Sierran and central + northern Sierran (i.e. *T. t. sierrae*) clusters each at one locus (*SODb* and *ACON2b*, respectively). The southern Californian population (population 1) did not possess any unique allozymes, though it was differentiated strongly from the coastal cluster (populations 3–17) at several loci. For example, at the *GDA* locus, allozyme *a* was fixed in San Diego, and was found elsewhere only in San Luis Obispo County (population 8) at low frequency (12.5%).

All four clusters could also be distinguished from one another by several allozymes that showed substantial differentiation among clusters. The southern Californian population (population 1) and the coastal cluster (populations 3–17) had allozymes that were highly divergent at three loci: *PGD*, *IDH1*, and *CAH1*. At *PGD*, allozyme *c* was present at high frequency in populations 2–5 of the coastal cluster, yet was absent from the southern Californian population (population 1). At the *IDH1* locus, allozyme *a* was fixed in the southern Californian population (population 1), and was present at low frequency (19%) in population 3, yet was absent from any other population. Allozyme *a* of the *CAH1* locus was fixed in the southern Californian population and absent from the coastal cluster, yet was also found in populations in the Sierra Nevada (populations 18–20, 30, 38).

Southern Sierran populations possessed both *T. t. torosa* and *T. t. sierrae* allozymes, despite their phylogenetic placement within *T. t. torosa*. At the *ACON2* locus, allozyme *a* was fixed within *T. t. torosa* (including the southern Sierran clade), while allozyme *b* was fixed within *T. t. sierrae*. Similarly, at the *SOD* locus, the central Sierran cluster had a unique, fixed allozyme (*b*) that distinguished it from the southern Sierran clade (Appendix). Thus, these two loci (*ACON2*, *SOD*) suggest that the southern Sierra Nevada is distinct from *T. t. sierrae*. In contrast, *ADH1*, *GDA*, and *LA1* all possessed a unique, fixed allozyme that was shared by *T. t. sierrae* and the southern Sierran clade of *T. t. torosa*, while the coastal and southern Californian clades of *T. t. torosa* were fixed for a separate unique allozyme (Appendix).

Tan & Wake (1995) recognized distinct central and northern Sierra Nevadan clusters of *T. t. sierrae* on the basis of mtDNA cytochrome *b* sequence evidence. There was some evidence for allozymic differentiation between the two regions in the current study. For instance, the central Sierran cluster had a unique, fixed allozyme at the *SOD* locus, and an allozyme at the *PGM* locus (*a*) that was not found in the northern cluster. The northern Sierran cluster possessed a unique allozyme at the *PGD* locus that was present in all populations at a frequency of 45–50%, yet was absent from the central Sierran cluster, and two allozymes (*a, c*) at the PAP locus that were found in the northern Sierran cluster were absent from the central Sierran cluster.

Among-cluster divergence was reflected by Nei's (1978) D_N (Table 2). Between the southern Californian population and the southernmost population of the coastal cluster (population 3), $D_N = 0.113$. In contrast, the D_N between populations at the northern and southern limits of the coastal cluster (populations 3 to 17) was 0.019, a value almost six times lower. The southern Sierran cluster was genetically uniform, with $D_N < 0.001$ among all population comparisons. Between the southern and central Sierran clusters, $D_N = 0.148$, and between the southern Sierran cluster and the coastal cluster + southern Californian population, $D_N > 0.17$. The maximum divergence within the central Sierran cluster was $D_N = 0.097$, the maximum divergence within the northern Sierran cluster was $D_N = 0.073$, and between the central and northern Sierran clusters D_N was 0.093.

Isolation by distance

Figure 5A shows the patterns of IBD for allozyme variation within the coastal and southern Sierran clades of *T. t. torosa*, and within *T. t. sierrae*. Allozyme frequencies were virtually identical in the southern Sierran clade, and there was no pattern of IBD ($D_N < 0.001$ among all population comparisons). The

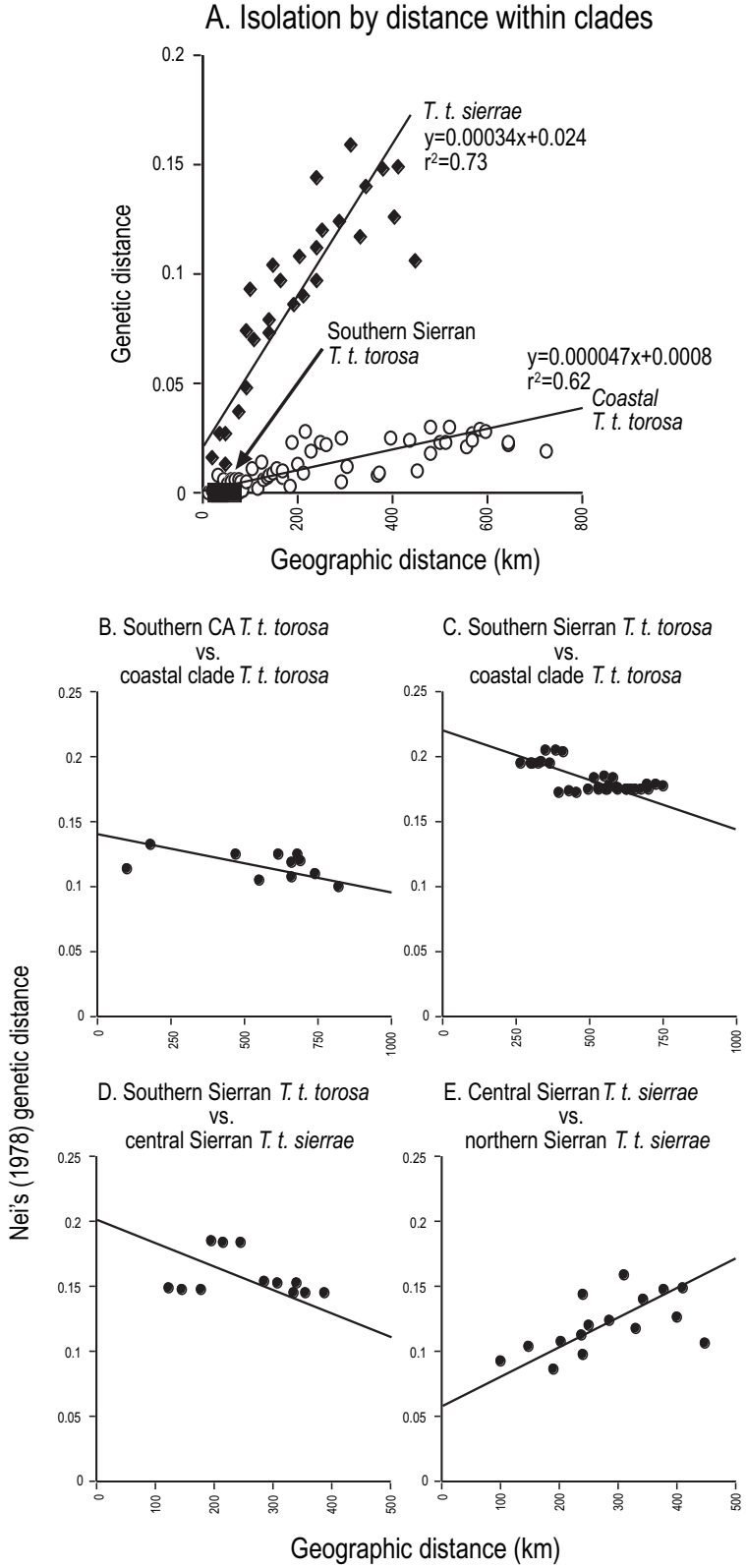

Figure 5. Isolation by distance plots. A, relationship between geographical distance (km) and genetic distance (Nei, 1978) within coastal *Taricha torosa torosa* (○), southern Sierran *T. t. torosa* (■), and *T. t. sierrae* (◆). B–E, relationship between geographical and genetic distances for comparisons between regions. In all cases, lines are reduced major axis regression.

coastal clade showed a significant pattern of IBD (Mantel test: $P = 0.001$; $r^2 = 0.73$), as did the *T. t. sierrae* clade (Mantel test: $P < 0.001$; $r^2 = 0.62$) (Fig. 5A). Populations showed more differentiation per unit distance in *T. t. sierrae* than in the coastal clade of *T. torosa* (Fig. 5A): the 99% confidence interval of the IBD slope was 0.00018–0.00045 for *T. t. sierrae*, and 0.000015–0.000071 for the coastal clade of *T. t. torosa*. These were nonoverlapping and thus significantly different.

Figure 5B–E shows the relationships between geographically adjacent regions. Comparing the southern Californian population with the coastal clade of *T. t. torosa*, genetic distance decreased with increasing geographical distance, and the *y*-intercept was $D_N = 0.14$ (Fig. 5B). Comparing the coastal and southern Sierran clades of *T. t. torosa*, genetic distance also decreased with increasing geographical distance, and the *y*-intercept was $D_N = 0.22$ (Fig. 5C). Comparing the southern Sierran clade of *T. t. torosa* with the central Sierran populations of *T. t. sierrae* (populations 30–34), the slope of RMA regression was again negative, and the *y*-intercept was at $D_N = 0.20$ (Fig. 5D). Unlike the other comparisons (Fig. 5B–D), comparison of the central and north Sierran clusters of *T. t. sierrae* showed a positive correlation between genetic and geographical distance (Fig. 5E); the *y*-intercept was $D_N = 0.06$.

Regional diversity: cytochrome *b*

Patterns of regional sequence diversity were estimated with mismatch distributions, haplotype networks, and diversity indices. A mismatch distribution of all *T. torosa* populations, including *T. t. torosa* and *T. t. sierrae*, was strongly bimodal (Fig. 6A), and differed significantly from a stepwise expansion model ($P = 0.04$). The peak on the left of Figure 6A (low *x*-axis values) displays comparisons within *T. t. torosa* (including the southern Sierra Nevadan populations) and within *T. t. sierrae*; the peak on the right (high *x*-axis values) is the outcome of comparisons between the two subspecies.

A mismatch distribution of the subspecies *T. t. torosa* (Fig. 6B) was weakly bimodal but not significantly different from that expected under an expansion model ($P > 0.05$). When only the coastal clade of *T. t. torosa* was considered (populations 5–17), the resulting mismatch distribution was similar to an expanding population (Fig. 6C). A haplotype network (Fig. 7A) showed a region of genetic uniformity in the San Francisco Bay region (populations 12–17), where seven sequences from five counties had identical mtDNA haplotypes. A mismatch distribution could not be calculated for the San Francisco Bay region due to the absence of nucleotide variation, but this lack of diversity suggests a recent colonization of the region. Haplotype diversity (h) and sequence diversity (κ) were lower in the coastal clade than in the southern Californian and southern Sierran clades (Table 3).

In contrast with the coastal clade, the southern Californian clade of *T. t. torosa* (populations 1–4) had a mismatch distribution (Fig. 6D) that differed significantly from that expected under an expansion model ($P = 0.02$). The haplotype network (Fig. 7A) was informative in its arrangement of the southern Californian clade, with the southernmost population in the southern Californian clade (population 1) more closely related to populations 8–9 than it was to populations 2–4. San Luis Obispo (population 7), Los Angeles (populations 5 and 6), and Monterey (population 10) were ambiguous in their relations (Fig. 7A).

Populations of the southern Sierran clade of *T. t. torosa* had a mismatch distribution consistent with an expanding population (Fig. 6E). A haplotype network linked the southern Sierran clade with coastal clade populations, but the source population was unclear, with the haplotype network showing connections to both Los Angeles and San Francisco Bay haplotypes (Fig. 7A).

The *T. t. sierrae* clade was trimodal in its mismatch distribution (Fig. 6F), and though it did not differ significantly from an expansion model, it approached significance ($P = 0.07$). The haplotype network (Fig. 7B) showed substantial structure, reflecting geographical relationships quite well, except for the lack of a connection between Calaveras and Mariposa counties. Sequence diversity (κ) and nucleotide diversity (π) were higher in *T. t. sierrae* (7.261, 0.022, respectively) than they were in *T. t. torosa* (3.735, 0.012); haplotype diversity (h) was similar in the two clades (Table 3). In addition, h, κ, and π measures were higher within both the central and the northern clades of *T. t. sierrae* than they were within any subclade of *T. t. torosa* (Table 3). Taken together, cytochrome *b* sequence variation was consistent with the allozyme data in suggesting that *T. t. sierrae* is more highly structured than is *T. t. torosa*.

Divergence times

Based on the average percent sequence divergence between clades, corrected for within-clade divergence, and assuming a rate of 0.8% sequence divergence per Myr at cytochrome *b* (Tan & Wake, 1995), *T. torosa* was estimated to have begun diverging in the Pliocene, with the split between *T. t. torosa* and *T. t. sierrae* dating to 7–13 Mya (pairwise sequence divergence/ML estimate of sequence divergence). Within *T. t. sierrae*, the northern and central Sierran clades diverged from one another roughly 2.6–3.4 Mya. Within *T. t. torosa*, populations colonized the southern Sierra Nevada 1.4–1.7 Mya. In southern California, the southern Californian clade and coastal

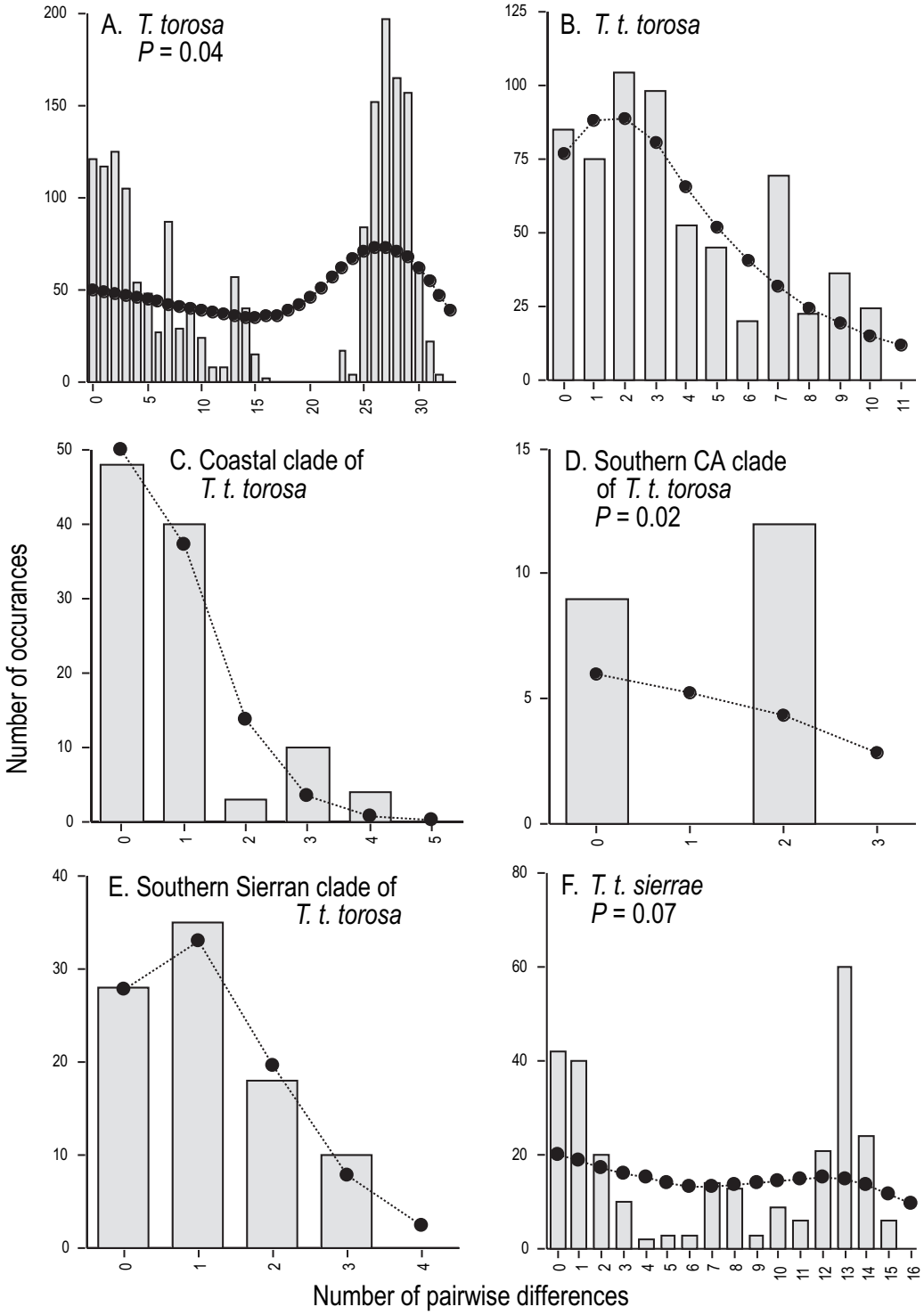

Figure 6. Mismatch distributions among haplotypes for: (A) all populations within *Taricha torosa* (including *T. t. torosa* and *T. t. sierrae*); (B) all populations of *T. t. torosa*; (C) populations in the coastal clade of *T. t. torosa* from Lake to Los Angeles Counties (populations 5–17); (D) southern California populations of *T. t. torosa* (populations 1–4); (E) southern Sierran populations (populations 18–25) of *T. t. torosa*; (F) all populations within *T. t. sierrae* (populations 26–39). Bars show the observed values; filled circles are expected values under a stepwise expansion model. Based on parametric bootstrap replicates (10 000), observed and expected values differ significantly for (A) ($P = 0.04$) and (D) ($P = 0.02$); (F) approaches significance ($P = 0.07$).

Table 3. Diversity indices of mtDNA cytochrome *b* sequences

Grouping	No. pops	No. individuals	No. usable base pairs[1]	No. poly sites	*h*	κ	π
Taricha torosa	37	60	304	44	0.911	15.012	0.049
T. t. torosa	23	36	315	15	0.865	3.735	0.012
Coastal Clade	11	15	331	5	0.543	0.876	0.003
Southern Californian clade	4	7	357	2	0.571	1.143	0.003
Southern Sierran Clade	8	14	327	4	0.692	1.110	0.003
T. t. sierrae	14	24	323	21	0.87	7.261	0.022
Central Sierran Region	9	17	323	17	0.787	4.794	0.015
Northern Sierran Region	5	7	366	5	0.810	1.810	0.005

[1]Sites with missing data were excluded.
h, haplotype diversity; κ, sequence diversity; π, nucleotide diversity; poly, polymorphic; pops, populations.

clade were estimated to have diverged 1.9–2.3 Mya. Within the southern Californian clade, San Diego (population 1) and Orange County (population 2) populations were estimated to have diverged roughly 875 000 years ago, but the associated haplotypes differed by only two substitutions. At the northern end of the coastal clade, the San Francisco Bay area populations (populations 12–17) were estimated to have diverged from populations south of Monterey (populations 5–10) between 0.375 and 1.1 Mya, depending on which populations were designated the ancestral source (Fig. 7A).

DISCUSSION

Multiple levels of divergence were found in *T. torosa*, including deep (i.e. phylogenetic) and shallow (e.g. IBD) differentiation. Phylogenetic analysis of the allozyme and mtDNA datasets recovered two major clades. One corresponded to *T. t. torosa*, and was distributed throughout coastal California, as well as in the southern Sierra Nevada. The other clade identified *T. t. sierrae*, and included the central and northern Sierra Nevada and extreme southern Cascades (Fig. 1). The distribution of these clades contradicts customary taxonomy in that *T. t. sierrae* was previously considered to occupy the entire length of the Sierra Nevada (Twitty, 1942; Stebbins, 2003). The finding of populations of *T. t. torosa* in the southern Sierra Nevada was not anticipated prior to Tan & Wake (1995). A molecular clock estimated that *T. t. torosa* and *T. t. sierrae* diverged 7–13 Mya.

Biogeography and taxonomy of *T. t. torosa* in southern California

Phylogenetic analyses of the allozyme and mtDNA variation revealed, with varying levels of support, three genetically differentiated regions within *T. t. torosa*: coastal, southern Californian, and southern Sierran (Figs 2 and 3). However, the geographical border between southern Californian and the coastal clade was discordant between the two data types. According to the allozyme phylogeny, the coastal clade extends from Orange County (population 3) in the south to Lake County (population 17) in the north, with a disjunct southern Californian population (San Diego County, population 1) sister to this clade (Fig. 2). In contrast, the mtDNA phylogeny supported the monophyly of a more northerly distributed southern Californian clade, including populations in San Diego (populations 1 and 2), Orange (population 3), and western Riverside (population 4) Counties (Fig. 3). The southern limit of the coastal mtDNA clade was located in Los Angeles County (populations 5 and 6). In the allozyme data, Nei's (1978) D_N between the San Diego (population 1) and Orange County (population 3) populations was 0.113, while the Los Angeles (population 6) and Orange County (population 3) populations were nearly genetically identical ($D_N = 0.001$). Our sample sizes were moderate, but it is unlikely that random sampling error was responsible for the discordance between the allozyme and mtDNA datasets. In the mtDNA dataset, the monophyly of the southern Californian clade, including populations from San Diego, Orange, and Riverside counties, was supported statistically with high bootstrap (91%) and posterior probability (99%) values. With the allozyme data, our sample sizes ranged from three to ten individuals (Table 1), but Nei (1978) has shown that, when genetic distances are large, small sample sizes can be compensated for by large numbers of loci. We examined 45 loci in this study (Appendix). Thus, while it would be unwise to compare weakly differentiated populations (e.g. among coastal clade populations), the larger genetic

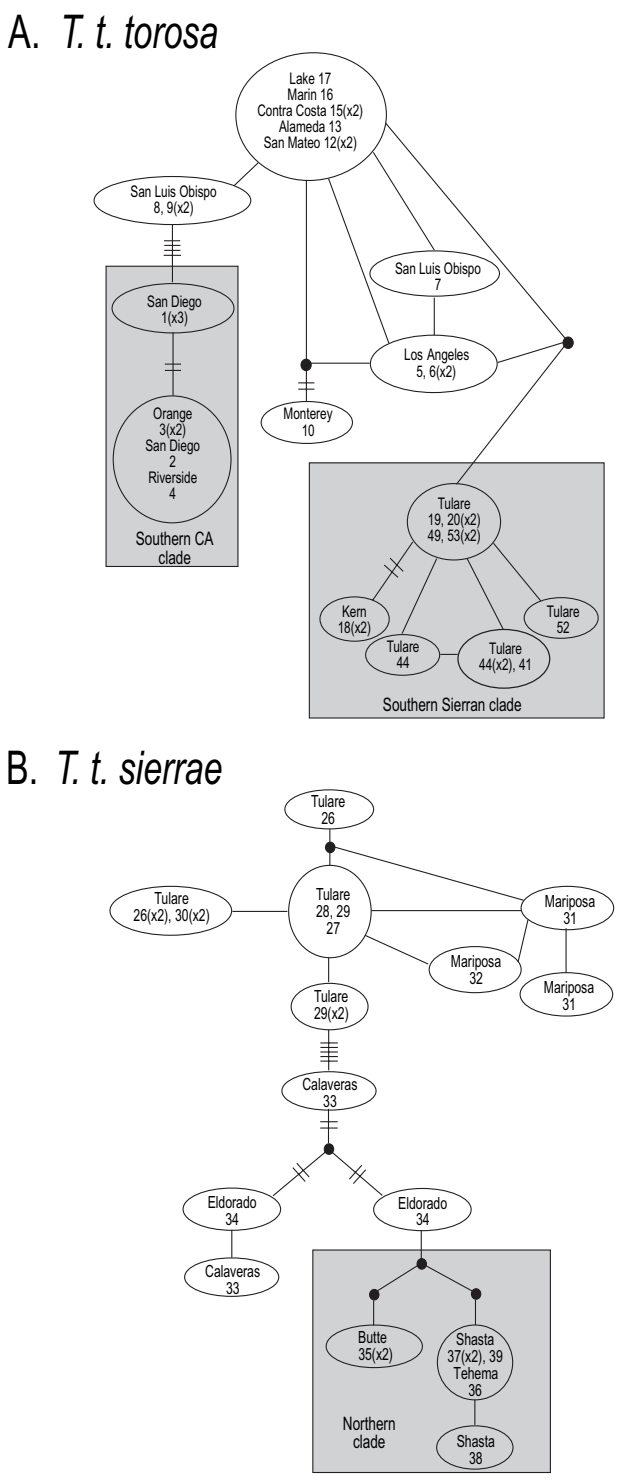

Figure 7. A, statistical parsimony haplotype network of all populations of *Taricha torosa torosa*. Lines between circles are one mutational step; when more than one mutation separates populations the number of hatch marks is the number of mutational steps. Black dots are inferred but unsampled haplotypes. The grey boxes highlight the southern Sierran clade and the southern Californian clade; the coastal clade is unshaded (Fig. 3). The counties and population numbers of haplotypes are provided (Table 1, Fig. 1). B, haplotype network of all populations of *T. t. sierrae*. The northern clade is shaded; populations in the central Sierran clade are unshaded.

distances, such as those between the coastal clade (populations 3–17) and the southern Californian population (population 1), were very likely real (other instances of relatively large genetic distances are discussed below).

Joint consideration of the allozyme and mtDNA datasets allowed for a refined biogeographical scenario for populations inhabiting southern California. A molecular clock estimate based on mtDNA variation dated the split between the southern Californian clade and the coastal clade at 1.9–2.3 Mya. A haplotype network (Fig. 7A) indicated the southernmost San Diego population (population 1) to be nested between coastal clade (populations 8 and 9) and southern clade (populations 2–4) populations, all of which were located to the north of population 1. This suggests that there existed a refugium in the vicinity of the southern limit of the range (e.g. population 1), followed by northward range expansion (Fig. 8A). A molecular clock dated this event at roughly 875 000 years ago. Subsequent range shifts, perhaps as a result of Pleistocene climate change, again isolated newts in the south, but demographically connected the populations to the north (i.e. populations 2–4 with 5 and 6) (Fig. 8B). Nuclear gene flow promoted genetic merger among these populations, yet the mtDNA remains as a relict of the historical association of populations 2–4 with population 1 (Fig. 8C). In the geographically disjunct populations to the south, genetic drift and perhaps natural selection generated genetic divergence at nuclear loci.

Discordances among datasets are interesting because of what they reveal about the evolutionary process. Consider the conflict discussed above between the allozyme and mtDNA data in *T. t. torosa* in southern California (populations 2–4). Such a situation could be caused by natural selection, lineage sorting, genetic drift, or reticulate evolution, and may be common near and below the species boundary (Ruedi, Smith & Patton, 1997; Maddison, 1997; Ballard & Whitlock, 2004). Discordance between allozyme and mtDNA borders has been documented in several salamander species, including plethodontids and salamandrids (García-París *et al*., 2003; Wake & Schneider, 1998; Mead, Tilley & Katz, 2001; Jockusch & Wake, 2002; Kuchta & Tan, 2005). This suggests that shared features, such as male-biased dispersal and the slow

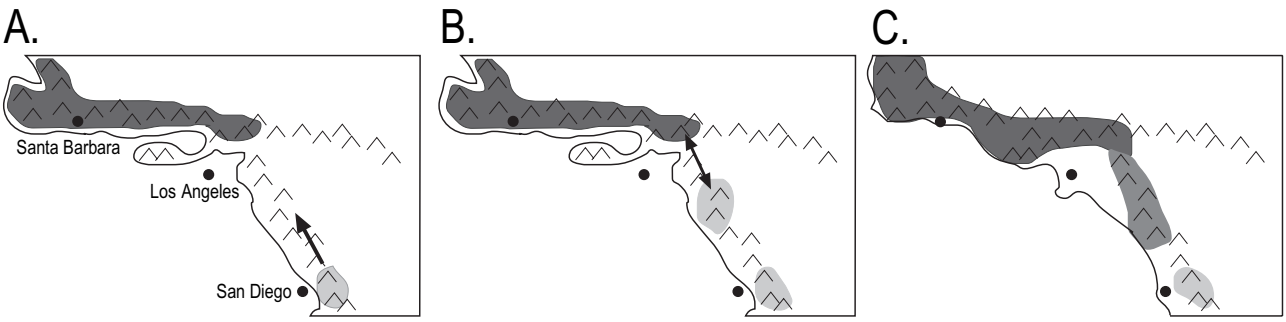

Figure 8. Biogeographical scenario for *Taricha torosa* in southern California. A, map of southern California from 2.5 to 0.5 Mya (based on Vedder & Howell, 1980; Hall, 2002). Populations in the north (dark grey shading) and south (light grey shading) were separated 2.3–1.9 Ma. By 875 000 years ago, populations in the southern region had expanded northward. B, coastal populations to the north and populations derived from the southern California region contact. Southern populations are again isolated in present-day San Diego County. C, present-day distribution of *T. torosa* in southern California. The region with intermediate shading has mtDNA that is related to populations in the south, but an allozyme profile that is closely related to populations to the north.

evolution of reproductive isolation, may be facilitate the evolution of discordances among datasets. Jockusch & Wake (2002), reporting on mtDNA and allozyme variation in the salamander genus *Batrachoseps*, make the case that mtDNA is often a remnant of deeper history, while allozymes are more informative regarding ongoing demographic interactions. Many discordances between allozyme and mtDNA data types are identified in *Batrachoseps*, and these are hypothesized to be the result of male-mediated gene flow promoting the merger of once-allopatric groups; mtDNA, in contrast, because of its maternally inherited nature and because females are highly philopatric, is more geographically stationary. Female philopatry may greatly extend the expected coalescence times of mtDNA lineages among subpopulations, because it results in small amounts of mtDNA gene flow (Hudson, 1990). A similar geographical discordance between mtDNA and allozymes was found in the Plethodontid salamander genus *Ensatina* (Jackman & Wake, 1994; Alexandrino *et al*., 2005), which exhibits a tension zone in allozyme frequencies about 50 km north of the contact zone between mtDNA clades (Moritz *et al*., 1992). Male-mediated gene flow and relative female philopatry may have been the demographic cause of this discordance as well, as male *Ensatina* move larger distances on average than do females (Staub, Brown & Wake, 1995). Male-mediated gene flow could also be responsible for the mtDNA/allozymic discordance in *T. torosa* in southern California. Trenham (1998) has shown at a study site in coastal California that *T. t. torosa* males move more frequently between breeding ponds than do females.

Earlier workers (Wolterstorff, 1935; Bishop, 1943) recognized the disjunct populations of newts in central San Diego county as a distinct species, but the distinctive morphological features (a 'warty' phenotype) were later determined to be the result of pathology (Brattstrom & Warren, 1953). Riemer (1958) found the San Diego populations to be divergent morphometrically, but he did not remove warty newts from his sampling, and thus his evidence for the morphometric distinctiveness of the San Diego newts is dubious. The genetic data presented here do not support long-term evolutionary independence of the San Diego populations from the remainder of the coastal cluster. The mtDNA divergence between the southern Californian and coastal clades was shallow and discordant with the allozymic pattern. In addition, no unique allozymes were identified in the southern population (population 1), despite the distinctiveness of its allozyme profile. Thus, at this time populations in the Cayumaca mountains are best considered conspecific with coastal populations. Nevertheless, populations in the Cayumaca mountains are genetically differentiated, demographically independent, geographically disjunct, and have a history of isolation relative to the coastal populations. They therefore constitute a distinct unit for conservation (Moritz, 1994). This is important, because current populations in southern California are small and seriously negatively affected by development and a number of ecological factors (reviewed in Kuchta, 2005).

BIOGEOGRAPHY OF *T. T. TOROSA* IN THE COAST RANGES OF CALIFORNIA

Allozymic evidence identified slight differentiation within the coastal cluster: $D_N = 0.019$ between Orange (population 3) and Lake County (population 17),

located at either end of the distribution. Despite the low level of differentiation, the relationship of genetic distance to geographical distance was consistent with IBD (Fig. 5A). As with the allozyme variation, mtDNA divergence was low, with haplotypes differing by a maximum of 4 bp (Fig. 7A). A mismatch distribution of all mtDNA haplotypes from Orange to Monterey County was consistent with an expansion model (Fig. 6C), and populations north of Monterey (population 10) shared a single haplotype (Fig. 7A).

These results suggest that coastal California was colonized via two separate expansion events. The first expansion spread from southern California to Monterey County. Prior to the Pliocene, the coast ranges of central California were not connected to the remainder of California, but existed as islands rising out of the Pacific (Yanev, 1980). During the Pliocene, uplift of the Tremblor range connected the Santa Ynez mountains in the south to the Gabilan and Santa Lucia Ranges, and the coast ranges south of Monterey were thus formed 5–3 Mya (Sims, 1993; Hall, 2002). This is the earliest that populations of *T. torosa* could have expanded northward to the present-day Monterey region, though this could have occurred later. Dispersal northward of Monterey, however, was impeded by the vast drainage of an inland sea in the present-day Central Valley (Yanev, 1980; Dupré, 1990; Sims, 1993). Beginning 2 Mya, continuing uplift of the Coast Ranges (especially the Diablo Range) closed the outlet of the marine seaway (Sarna-Wojcicki *et al*., 1985), and the Central Valley filled with fresh water, which drained out through the modern Salinas and Pajaro river valleys. Finally, 600 000 years ago, further uplift shifted the drainage of the Central Valley northward through the present-day Carquinez Strait and out the Golden Gate (Sarna-Wojcicki *et al*., 1985). A complete lack of mtDNA variation and limited allozyme variation north of Monterey County suggests that *T. t. torosa* only recently expanded northward from the Monterey region (Fig. 1). Application of a molecular clock indicated that this occurred between 0.375 and 1.1 Mya, which is consistent with known geological events.

The Monterey Bay region is an influential biogeographical barrier that has strongly impacted on the biogeography of many taxa with limited capacity to disperse across marine barriers. Many Pacific north-west salamanders have their southernmost limit at or near this barrier, including the long-toed salamander (*Ambystoma macrodactylum*), Pacific giant salamander (*Dicamptodon ensatus*), black salamander (*Aneides flavipunctatus*), Oregon salamander (*E. eschscholtzii oregonensis*), California slender salamander (*Batrachoseps attenuatus*), and the rough-skinned newt (*T. granulosa*). Other species reach their northern limit near Monterey Bay, including the Monterey salamander (*E. e. eschscholtzii*), the Santa Lucia Mountains slender salamander (*B. luciae*), and the Gabilan Mountains slender salamander (*B. gabilanensis*). The yellow-eyed salamander (*E. e. xanthoptica*) has a distribution similar to that of *T. t. torosa* north of Monterey Bay, and the Monterey Bay drainage may have been a barrier separating *E. e. oregonensis* from *E. e. eschscholtzii* and *E. e. xanthoptica* (Wake, 1997). Finally, the arboreal salamander (*An. lugubris*), though distributed north of Monterey Bay, has a mtDNA diversity pattern indicating that Monterey Bay was a barrier in this species as well, with northward expansion following closure of the seaway (Jackman, 1993), as with *T. t. torosa*. Note that two salamander species that originated south of Monterey Bay have expanded northward, but no salamander species originating in the north have moved southward. This may be due to habitat differences north and south of Monterey Bay. Aside from isolated pockets of habitat, the northern end of Monterey Bay marks the southern extent of coniferous forest. In contrast, drier oak woodland and chaparral is common south of Monterey bay, and these habitat types extend northward on the inland side of the coast ranges. Consistent with this interpretation, *T. torosa* populations north of Monterey Bay have an inland distribution, while populations south of Monterey are distributed coastally (Fig. 1).

Biogeography of *T. t. torosa* in the southern Sierra Nevada

Allozyme diversity within the southern Sierran clade was quite limited; Nei's D_N was < 0.001 between all population comparisons (Table 2). In addition, a mtDNA mismatch distribution for the southern Sierra Nevadan clade fitted the predictions of a range expansion model (Fig. 6E). These results are consistent with the populations colonizing the Sierra Nevada undergoing a founder event that severely reduced genetic diversity. The close relationship of southern Sierran haplotypes to the coastal clade of *T. t. torosa* (Fig. 7A) suggests that this colonization was recent, 1.4–1.7 Mya according to a molecular clock. In contrast to the lack of allozyme diversity within the clade, Nei's D_N between the southern clade and the coastal clade was high, around 0.20. Three loci possessed unique, fixed allozymes in the southern Sierran clade (*AAT1*, *EST2*, *CA2*) (Appendix). These may be newly evolved, though they could represent low-frequency allozymes located elsewhere (our sample sizes were not sufficient to detect rare allozymes reliably: Rannala, 1995; Wiens & Servedio, 2000). It is also interesting to note that three loci (*ADH1*, *GDA*, and *LA1*) had allozymes that were fixed in both *T. t. sierrae* and the southern Sierran clade of *T. t. torosa*, but were absent from the

coastal and southern Californian clades of *T. t. torosa*. These loci are candidates for adaptive spread across the contact zone between *T. t. torosa* and *T. t. sierrae*, though much more research and larger samples are required to determine this.

As with *T. torosa*, other taxa have been found in which the southern Sierra Nevada is occupied by a lineage related more closely to lineages in southern California or the coast ranges than to those in the remainder of the Sierra Nevada. Examples include, among others, the frog *Rana muscosa* (Macey *et al*., 2001), the salamander *E. eschscholtzii* (Moritz *et al*., 1992; Jackman & Wake, 1994) and the woodrat, *Neotoma fuscipes* (Matocq, 2002). This pattern has been identified and summarized by Macey *et al*. (2001) and Calsbeek *et al*. (2003). However, a specific geological or climatic explanation has yet to be identified.

Divergence within *T. t. sierrae* in the Sierra Nevada

Taricha t. sierrae was found to be highly divergent genetically, with higher levels of allozymic (Fig. 4) and mtDNA (Table 2) differentiation than in any other clade of *T. t. torosa*. IBD in allozymes was also significantly stronger in *T. t. sierrae* than in *T. t. torosa* (Fig. 5A). The increased differentiation within *T. t. sierrae* relative to *T. t. torosa* may be a consequence of the topographical and geological complexity of the Sierra Nevada, which has high elevation ridges separating major river valleys, reducing the demographic connectedness among populations. In addition, in contrast to the coast ranges, the Sierra Nevada is well over 50 Myr old (House *et al*., 1998; Wakabayashi & Sawyer, 2001) and thus predates the *T. t. sierrae* lineage. The data suggest that *T. t. sierrae* has been a long-term occupant of the Sierra Nevada.

Based on mtDNA sequence data, Tan & Wake (1995) recognized two genetic groups within *T. t. sierrae*, corresponding to the northern and central regions of the Sierra Nevada. The current phylogenetic analysis of the mtDNA data also portrayed monophyletic northern and central clades, though they lacked solid statistical support (Fig. 3). In a phylogenetic analysis of the allozyme data, the northern clade was monophyletic (bootstrap support = 70%; DI = 3); however, the central clade was paraphyletic and was poorly supported statistically (Fig. 2). IBD in allozymes was found between the central and northern regions, but the *y*-intercept was greater than zero ($D_N = 0.06$), indicating that the two regions are more genetically divergent than IBD alone would predict (Fig. 5E). Thus, the above analyses suggest some degree of historical or demographic separation between central and northern Sierran populations of *T. t. sierrae*. However, there is also a large amount of differentiation within the central and northern regions. For example, in the mtDNA data, haplotype, sequence, and nuclear diversity were higher within the central and northern clades of *T. t. sierrae* than they were within either the coastal, southern Californian, or southern Sierran clades of *T. t. torosa* (Table 3). Additionally, an MDS analysis of the allozyme data failed to show the central and northern regions as discrete: some between-region Euclidean distances were shorter than were many within-region distances. Taken together, the results of this study suggest that *T. t. sierrae* is best considered as a highly differentiated evolutionary unit rather than two discrete, evolutionarily independent lineages.

CONCLUSIONS

Using molecular genetic tools, we inferred the phylogeographical history of the California newt, *T. torosa*. The history is complex, including allopatric divergence among lineages, IBD within geographical regions, and range expansion into new terrains. These results are consistent with what is understood of the elaborate geomorphological evolution of the California landscape. Our approach to phylogeography integrated a diversity of phylogenetic and population genetic methods for exploring deep and shallow time depths. We also included both mtDNA sequence data and nuclear allozyme data, and in some instances the two datasets recorded discordant signals. By including multiple marker types, understanding of the phylogeography of *T. torosa* was refined and improved. We thus suggest that workers should be cautious about making phylogeographical inferences on the basis of a single data type, and we agree with Moritz *et al*. (1992) that mtDNA data alone should not be used to diagnose species.

We have shown that the distributional ranges of *T. t. torosa* and *T. t. sierrae* are different from those previously thought, with populations in the southern Sierra Nevada being most closely related to coastal *T. t. torosa*. Because *T. t. torosa* and *T. t. sierrae* are monophyletic lineages, with deep mtDNA and allozymic divergence, and because the lineages are relatively old, some workers may recognize two separate species. However, work on the systematics of *T. torosa* continues, including a study of the contact zone between *T. t. torosa* and *T. t. sierrae* in the vicinity of the Kaweah River in Tulare County, California (Fig. 1). In the interests of taxonomic stability, we withhold judgement on the taxonomy of *T. t. sierrae* and *T. t. torosa* until the ongoing work is completed (S. Kuchta, unpubl. data).

ACKNOWLEDGEMENTS

Numerous government agencies allowed us or others to collect specimens for this research, and their support is appreciated. Valuable specimens and/or field support were provided to us by R. Fisher, G. Fellers, W. Guo, R. Hansen, D. Holland, B. Leonard, C. Luke, D. Morafka, B. Norman, T. Pappenfuss, R. Sage, N. Staub, D. Wake and E. Zhao. This research was in part funded by the NSF grant DEB 0072869 to D.B. Wake and S.R.K., and S.R.K. was supported by an NSF Predoctoral Fellowship and NSF grant DEB 0317182 to B. Sinervo and S.R.K. The work of A.T. was funded by a Carl B. Koford grant (Museum of Vertebrate Zoology, U.C. Berkeley), and the Department of Integrative Biology (U.C. Berkeley). This manuscript was greatly improved by comments from Ammon Corl, Jim Kurpius, Erica Rosenblum, and David Wake. Both authors thank our thesis committees and D. B. Wake for his generous guidance and support.

REFERENCES

Alexandrino J, Baird SJE, Lawson L, Macey JR, Moritz C, Wake DB. 2005. Strong selection against hybrids at a hybrid zone in the *Ensatina* ring species complex and its evolutionary implications. *Evolution* **59:** 1334–1347.

Avise JC. 2000. *Phylogeography: the history and formation of species*. Cambridge, Massachusetts: Harvard University Press.

Avise JC, Walker D. 1998. Pleistocene phylogeographic effects on avian populations and the speciation process. *Proceedings of the Royal Society of London, Series B* **265:** 457–463.

Ballard JWO, Whitlock MC. 2004. The incomplete natural history of mitochondria. *Molecular Ecology* **13:** 729–744.

Bishop SC. 1943. *A handbook of salamanders*. Ithaca, New York: Comstock Publishing.

Bohonak AJ. 2002. IBD 1.52 (isolation by distance): a program for population genetic analyses of isolation by distance. *Journal of Heredity* **93:** 153–154.

Bohonak AJ. 2004. *RMA 1.16: software for reduced major axis regression.* http://www.bio.sdsu.edu/pub/andy/rma.html.

Brattstrom BH, Warren JW. 1953. On the validity of *Taricha torosa klauberi* Wolterstorff. *Herpetologica* **9:** 180–182.

Bremer K. 1994. Branch support and tree stability. *Cladistics* **10:** 295–304.

Brunsfeld SJ, Sullivan J, Soltis DE, Soltis PS. 2001. Comparative phylogeography of northwestern North America: a synthesis. In: Silvertown J, Antonovics F, eds. *Integrating ecology and evolution in a spatial context*. Oxford: Blackwell Science, 319–339.

Calsbeek R, Thompson JN, Richardson JE. 2003. Patterns of molecular evolution and diversification in a biodiversity hotspot: the California Floristic Province. *Molecular Ecology* **12:** 1021–1029.

Carstens BC, Stevenson AL, Degenhardt JD, Sullivan J. 2004. Testing nested phylogenetic and phylogeographic hypotheses in the *Plethodon vandykei* species group. *Systematic Biology* **55:** 781–792.

Clement M, Posada D, Crandall KA. 2000. TCS: a computer program to estimate gene genealogies. *Molecular Ecology* **9:** 1657–1660.

Dupré WR. 1990. Quaternary geology of the Monterey Bay region, California. In: Garrison RE, ed. *Geology and tectonics of the Central California coast region, San Francisco to Monterey*. Pacific Station: Society for Economic Paleontology and Mineralogy, 185–191.

Felsenstein J. 1982. How can we infer geography and history from gene frequencies? *Journal of Theoretical Biology* **96:** 9–20.

Felsenstein J. 1985. Confidence limits on phylogenies: an approach using the bootstrap. *Evolution* **39:** 783–791.

García-París M, Alcobendas M, Buckley D, Wake DB. 2003. Dispersal of viviparity across contact zones in Iberian populations of Fire salamanders (*Salamandra*) inferred from discordance of genetic and morphological traits. *Evolution* **57:** 129–143.

Good DA, Wake DB. 1992. Geographic variation and speciation in the Torrent Salamanders of the genus *Rhyacotriton* (Caudata: Rhyacotritonidae). *University Of California Publications in Zoology* **126:** 1–91.

Hall CA Jr. 2002. Nearshore marine paleoclimatic regions, increasing zoogeographic provinciality, molluscan extinctions, and paleoshores, California: late Oligocene (27 Ma) to late Pliocene (2.5 Ma). *Geological Society of America, Special Paper* **357:** v–489.

Hasagawa M, Kishino H, Yano T. 1985. Dating of the human-ape splitting by a molecular clock of mitochondrial DNA. *Journal of Molecular Evolution* **22:** 160–174.

Hellberg ME. 1994. Relationships between inferred levels of gene flow and geographic distance in a philopatric coral, *Balanophyllia elegans*. *Evolution* **48:** 1829–1854.

Hillis DM, Moritz C, Mable BK. 1996. Applications of molecular systematics: the state of the field and a look to the future. In: Hillis DM, Moritz C, Mable BK, eds. *Molecular systematics*, 2nd edn. Sunderland, Massachusetts: Sinauer Associates, Inc, 515–543.

House MA, Wernicke BP, Farley KA. 1998. Dating topography of the Sierra Nevada, California, using apatite (U-Th) ages. *Nature* **396:** 66–69.

Hudson RR. 1990. Gene genealogies and the coalescent process. *Oxford Surveys in Evolutionary Biology* **7:** 1–44.

Huelsenbeck JP, Ronquist F. 2001. MRBAYES: Bayesian inference of phylogenetic trees. *Bioinformatics* **17:** 754–755.

Jackman TR. 1993. Evolutionary and historical analyses within and among members of the salamander tribe Plethodontini (Amphibia: Plethodontidae). Unpubl. PhD Thesis, University of California, Berkeley.

Jackman TR, Wake DB. 1994. Evolutionary and historical analysis of protein variation in the blotched forms of salamanders of the *Ensatina* complex (Amphibia: Plethodontidae). *Evolution* **48:** 876–897.

Jockusch EL, Wake DB. 2001. Molecular phylogenetic analysis of slender salamanders, genus *Batrachoseps* (Amphibia: Plethodontidae), from coastal California with descriptions of four new species. *Herpetological Monographs* **15:** 54–99.

Jockusch EL, Wake DB. 2002. Falling apart and merging: diversification of slender salamanders (Plethodontidae: *Batrachoseps*) in the American West. *Biological Journal of the Linnaean Society* **76:** 361–391.

Kuchta SR. 2002. *Systematics, speciation, and mimicry in Taricha (Caudata: Salamandridae)*. Unpubl. PhD Thesis, University of California, Berkeley.

Kuchta SR. 2005. *Taricha torosa*. In: Lannoo M, ed. *Status and conservation of U.S. amphibians*. Washington DC: Smithsonian Institution Press, 904–908.

Kuchta SR, Meyer D. 2001. A genealogical view of geographical variation. *Molecular Ecology* **10:** 2569–2576.

Kuchta SR, Tan AM. 2005. Isolation by distance and postglacial range expansion in the Rough-skinned newt, *Taricha granulosa*. *Molecular Ecology* **14:** 225–244.

Larget B, Simon DL. 1999. Markov chain Monte Carlo algorithms for the Bayesian analysis of phylogenetic trees. *Molecular Biology and Evolution* **16:** 750–759.

Larson A, Weisrock DW, Kozak KH. 2003. Phylogenetic systematics of salamanders (Amphibia: Urodela), a review. In: Sever DM, ed. *Reproductive Biology and Phylogeny of the Urodela*. Enfield, New Hampshire: Science Publishers, Inc., 31–108.

Lessa EP. 1990. Multidimensional analysis of geographic genetic structure. *Systematic Zoology* **39:** 242–252.

Lewis PO. 2001. Phylogenetic systematics turns over a new leaf. *Trends in Ecology and Evolution* **16:** 30–37.

Mabee PM, Humphries J. 1993. Coding polymorphic data: examples from allozymes and ontogeny. *Systematic Biology* **42:** 166–181.

Macey JR, Strasburg JL, Brisson JA, Vredenburg VT, Jennings M, Larson A. 2001. Molecular phylogenetics of western North American frogs of the *Rana boylii* species group. *Molecular Phylogenetics and Evolution* **19:** 131–143.

Maddison WP. 1997. Gene trees in species trees. *Systematic Biology* **46:** 523–536.

Mahoney MJ. 2004. Molecular systematics and phylogeography of the *Plethodon elongatus* species group: combining phylogenetic and population genetic methods to investigate species history. *Molecular Ecology* **13:** 149–166.

Matocq MD. 2002. Phylogeographical structure and regional history of the dusky-footed woodrat, *Neotoma fuscipes*. *Molecular Ecology* **11:** 229–242.

Mead LS, Tilley SG, Katz LA. 2001. Genetic structure of the Blue Ridge Dusky Salamander (*Desmognathus orestes*): inferences from allozymes, mitochondrial DNA, and behavior. *Evolution* **55:** 2287–2302.

Mickevich MF, Mitter C. 1981. Treating polymorphic characters in systematics: a phylogenetic treatment of electrophoretic data. In: Funk VA, Brooks DR, eds. *Advances in Cladistics*, Vol. 1. New York: New York Botanical Garden, 169–176.

Moritz C. 1994. Defining 'evolutionary significant units' for conservation. *Trends in Ecology and Evolution* **9:** 373–375.

Moritz C, Schneider CJ, Wake DB. 1992. Evolutionary relationships within the *Ensatina eschscholtzii* complex confirm the ring species interpretation. *Systematic Biology* **41:** 273–291.

Murphy RW, Sites JW, Buth DG, Haufler CH. 1996. Proteins: isozyme electrophoresis. In: Hillis DM, Moritz C, Mable BK, eds. *Molecular systematics*. Sunderland, Massachusetts: Sinauer Associates Inc., 51–120.

Nei M. 1978. Estimation of average heterozygosity and genetic distance from a small number of individuals. *Genetics* **89:** 583–590.

Nei M. 1987. *Molecular evolutionary genetics*. New York: Columbia University Press.

Nylander JAAA. 2002. *MrModeltest.* http://www.ebc.uu.se/systzoo/staff/nylander.html

Petranka JW. 1998. *Salamanders of the United States and Canada*. Washington DC: Smithsonian Institution Press.

Poe S. 1998. Sensitivity of phylogeny estimation to taxonomic sampling. *Systematic Biology* **47:** 18–31.

Posada D, Crandall KA. 1998. Modeltest: testing the model of DNA substitution. *Bioinformatics* **14:** 817–818.

de Queiroz K, Good DA. 1997. Phenetic clustering in biology: a critique. *Quarterly Review of Biology* **72:** 3–30.

Rannala B. 1995. Polymorphic characters and phylogenetic analysis: a statistical perspective. *Systematic Biology* **44:** 421–429.

Riemer WJ. 1958. Variation and systematic relationships within the salamander genus *Taricha*. *University of California Publications in Zoology* **56:** 301–390.

Rogers JS. 1972. *Measures of genetic similarity and genetic distance. Studies in Genetics VII.* Austin, Texas: University of Texas Publication **7213:** 145–153.

Rozas J, Sánchez-DelBarrio JC, Messeguer X, Rozas R. 2003. DnaSP, DNA polymorphism analyses by the coalescent and other methods. *Bioinformatics* **19:** 2496–2497.

Ruedi M, Smith MF, Patton JL. 1997. Phylogenetic evidence of mitochondrial DNA introgression among pocket gophers in New Mexico (family Geomyidae). *Molecular Ecology* **6:** 453–462.

Sarna-Wojcicki AM, Meyer CE, Bowman HR, Hall NT, Russell PC, Woodward MJ, Slate JL. 1985. Correlation of the Rockland ash bed, a 400,000-year-old stratigraphic marker in northern California and western Nevada and implications for middle Pleistocene paleogeography of central California. *Quaternary Research* **23:** 236–257.

Schneider S, Excoffier L. 1999. Estimation of past demographic parameters from the distribution of pairwise differences when the mutation rates vary among sites: application to human mitochondrial DNA. *Genetics* **152:** 1079–1089.

Schneider S, Roessli D, Excoffier L. 2000. *Arlequin*, Vers. 2.001*: a software for population genetics data analysis.* Genetics and Biometry Laboratory, University of Geneva, Switzerland.

Sims JD. 1993. Chronology of displacement on the San Andreas fault in central California: evidence from reversed positions of exotic rock bodies near Parkfield, California. In: Powell RE, Weldon RJ, Matti JC, eds. *The San Andreas*

faulty system: displacement, palinspastic reconstruction, and geologic evolution. Boulder, Colorado: Geological Society of America Memoirs, Vol. **178,** 231–256.

Slatkin M. 1993. Isolation by distance in equilibrium and non-equilibrium populations. *Evolution* **47:** 264–279.

Slatkin M, Hudson RR. 1991. Pairwise comparisons of mitochondrial DNA sequences in stable and exponentially growing populations. *Genetics* **129:** 555–562.

Staub NL, Brown CW, Wake DB. 1995. Patterns of growth and movements in a population of *Ensatina eschscholtzii platensis* (Caudata: Plethodontidae) in the Sierra Nevada, California. *Journal of Herpetology* **29:** 593–599.

Stebbins RC. 2003. *A Field guide to western reptiles and amphibians*, 3rd edn. Boston, Massachusetts: Houghton Mifflin.

Swofford DL. 2002. *PAUP*. phylogenetic analysis using parsimony (* and other methods)*, Vers. 4.0b10. Sunderland, Massachusetts: Sinauer Associates.

Tan AM. 1993. *Systematics, phylogeny and biogeography of the northwest American newts of the genus Taricha (Caudata: Salamandridae)*. Unpubl. PhD Thesis, University of California, Berkeley.

Tan AM, Wake DB. 1995. MtDNA phylogeography of the California newt, *Taricha torosa* (Caudata, Salamandridae). *Molecular Phylogenetics and Evolution* **4:** 383–394.

Tilley SG, Mahoney MJ. 1996. Patterns of genetic differentiation in salamanders of the *Desmognathus ochrophaeus* complex (Amphibia: Plethodontidae). *Herpetological Monographs* **10:** 1–42.

Trenham PC. 1998. Demography, migration, and metapopulation structure of pond breeding salamanders. Unpubl. PhD Thesis, University of California, Davis.

Twitty VC. 1942. The species of Californian *Triturus*. *Copeia* **1942:** 65–76.

Vedder JG, Howell DG. 1980. Topographic evolution of the southern California borderland during late Cenozoic time. In: Power DM, ed. *The California islands.* Proceedings of a Multidisciplinary Symposium. Santa Barbara, California: Santa Barbara Museum of Natural History, 7–31.

Wakabayashi J, Sawyer TL. 2001. Stream incision, tectonics, uplift, and evolution of the topography of the Sierra Nevada, California. *Journal of Geology* **109:** 539–562.

Wake DB. 1997. Incipient species formation in salamanders of the *Ensatina* complex. *Proceedings of the National Academy of Sciences* **94:** 7761–7767.

Wake DB, Schneider CJ. 1998. Taxonomy of the plethodontid salamander genus *Ensatina*. *Herpetologica* **54:** 279–298.

Wiens JJ. 2000. Reconstructing phylogenies from allozyme data: comparing method performance with congruence. *Biological Journal of the Linnaean Society* **70:** 613–632.

Wiens JJ, Servedio MR. 2000. Species delimitation in systematics: inferring diagnostic differences between species. *Proceedings of the Royal Society of London, Series B* **267:** 631–636.

Wolterstorff W. 1935. Ueber eine eigentümliche Form des kalifornischen Wassermolches, *Taricha torosa* (Rathke). *Blätter für Aquarien und Terrarienkunde* **46:** 178–184.

Wright S. 1943. Isolation by distance. *Genetics* **28:** 114–138.

Yanev KP. 1980. Biogeography and distribution of three parapatric salamander species in coastal and borderland California. In: Power DM, ed. *The California islands.* Proceedings of a Multidisciplinary Symposium. Santa Barbara, California: Santa Barbara Museum of Natural History, 531–550.

APPENDIX

TARICHA TOROSA ALLOZYME FREQUENCIES

	T. t. torosa															*T. t. sierrae*							
Region:	SD	Coast Ranges											Southern Sierra Nevada			Central Sierra Nevada				Northern Sierra Nevada			
Pop:	1	3	6	9	10	11	12	13	14	15	16	17	18	19	20	30	31	33	34	35	36	37	38
n =	5	8	3	8	3	7	10	10	5	10	10	5	6	3	7	10	10	9	5	10	7	3	10
AAT1																							
b	–	–	–	–	–	–	–	–	–	–	–	–	1.000	1.000	1.000	–	–	–	–	–	–	–	–
c	1.000	1.000	1.000	1.000	1.000	1.000	1.000	1.000	1.000	1.000	1.000	1.000	–	–	–	0.700	1.000	0.500	–	–	–	–	–
d	–	–	–	–	–	–	–	–	–	–	–	–	–	–	–	0.300	–	0.500	1.000	1.000	1.000	1.000	1.000
ACON1																							
b	–	–	–	–	–	–	–	–	–	–	–	–	–	–	–	–	–	0.222	–	–	–	–	–
c	1.000	1.000	1.000	1.000	1.000	1.000	1.000	1.000	1.000	1.000	1.000	1.000	1.000	1.000	1.000	1.000	0.350	0.778	1.000	1.000	1.000	1.000	1.000
d	–	–	–	–	–	–	–	–	–	–	–	–	–	–	–	–	0.650	–	–	–	–	–	–
ACON2																							
a	1.000	1.000	1.000	1.000	1.000	1.000	1.000	1.000	1.000	1.000	1.000	1.000	1.000	1.000	1.000	–	–	–	–	–	–	–	–
b	–	–	–	–	–	–	–	–	–	–	–	–	–	–	–	1.000	1.000	1.000	1.000	1.000	1.000	1.000	1.000
ADA2																							
a	–	–	–	0.500	–	–	–	–	–	0.050	–	–	–	–	–	–	–	–	–	–	–	–	–
b	1.000	0.500	0.500	0.500	1.000	1.000	1.000	1.000	1.000	0.950	1.000	1.000	1.000	1.000	1.000	1.000	1.000	1.000	1.000	1.000	1.000	1.000	1.000
e	–	0.500	0.500	–	–	–	–	–	–	–	–	–	–	–	–	–	–	–	–	–	–	–	–
ADH1																							
a	1.000	1.000	1.000	1.000	1.000	1.000	1.000	1.000	1.000	1.000	1.000	1.000	–	–	–	–	–	–	–	–	–	–	–
b	–	–	–	–	–	–	–	–	–	–	–	–	1.000	1.000	1.000	1.000	1.000	1.000	1.000	1.000	1.000	1.000	1.000
CAH1																							
a	1.000	–	–	–	–	–	–	–	–	–	–	–	1.000	1.000	1.000	1.000	–	–	–	–	–	–	1.000
b	–	1.000	1.000	1.000	0.667	1.000	1.000	1.000	1.000	1.000	1.000	1.000	–	–	–	–	1.000	1.000	1.000	1.000	1.000	1.000	–
c	–	–	–	–	0.333	–	–	–	–	–	–	–	–	–	–	–	–	–	–	–	–	–	–
CAH2																							
a	–	–	–	–	–	–	–	–	–	–	0.100	–	–	–	–	–	–	0.222	0.200	–	–	–	–
b	1.000	1.000	1.000	1.000	1.000	1.000	1.000	1.000	1.000	1.000	0.900	1.000	–	–	–	1.000	1.000	0.778	0.800	1.000	1.000	1.000	1.000
c	–	–	–	–	–	–	–	–	–	–	–	–	1.000	1.000	1.000	–	–	–	–	–	–	–	–
EST2																							
b	1.000	1.000	1.000	1.000	1.000	1.000	1.000	1.000	1.000	1.000	1.000	1.000	–	–	–	–	–	1.000	1.000	–	–	–	–
c	–	–	–	–	–	–	–	–	–	–	–	–	–	–	–	1.000	1.000	–	–	1.000	1.000	1.000	1.000
d	–	–	–	–	–	–	–	–	–	–	–	–	1.000	1.000	1.000	–	–	–	–	–	–	–	–
GAPDH																							
a	–	–	–	–	–	–	–	–	–	–	–	–	–	–	–	0.600	0.444	–	–	–	0.667	0.667	0.500
b	1.000	1.000	1.000	0.750	0.667	0.571	0.600	0.667	0.600	0.600	1.000	1.000	1.000	1.000	1.000	0.400	0.556	1.000	1.000	1.000	0.333	0.333	0.500
c	–	–	–	0.250	0.333	0.429	0.400	0.333	0.400	0.400	–	–	–	–	–	–	–	–	–	–	–	–	–

APPENDIX *Continued*

	T. t. torosa															*T. t. sierrae*							
Region:	SD	Coast Ranges											Southern Sierra Nevada			Central Sierra Nevada				Northern Sierra Nevada			
Pop:	1	3	6	9	10	11	12	13	14	15	16	17	18	19	20	30	31	33	34	35	36	37	38
n =	5	8	3	8	3	7	10	10	5	10	10	5	6	3	7	10	10	9	5	10	7	3	10
GDA																							
a	1.000	–	–	0.125	–	–	–	–	–	–	–	–	–	–	–	–	–	–	–	–	–	–	–
b	–	1.000	1.000	0.875	1.000	1.000	1.000	1.000	1.000	1.000	1.000	1.000	–	–	–	–	–	–	–	–	–	–	–
c	–	–	–	–	–	–	–	–	–	–	–	–	1.000	1.000	1.000	1.000	1.000	1.000	1.000	1.000	1.000	1.000	1.000
GPI																							
a	1.000	1.000	1.000	1.000	1.000	1.000	1.000	1.000	1.000	1.000	1.000	1.000	0.917	1.000	1.000	1.000	1.000	0.889	1.000	0.150	1.000	1.000	1.000
b	–	–	–	–	–	–	–	–	–	–	–	–	0.083	–	–	–	–	0.111	–	0.850	–	–	–
IDH1																							
a	1.000	0.188	–	–	–	–	–	–	–	–	–	–	–	–	–	–	–	–	–	–	–	–	–
b	–	0.813	1.000	1.000	1.000	1.000	1.000	1.000	1.000	1.000	0.950	1.000	1.000	1.000	1.000	0.950	1.000	1.000	1.000	1.000	1.000	1.000	1.000
c	–	–	–	–	–	–	–	–	–	–	0.050	–	–	–	–	0.050	–	–	–	–	–	–	–
IDH2																							
a	–	–	–	–	–	–	–	–	–	–	–	–	–	–	0.143	–	–	–	–	–	–	–	–
b	1.000	1.000	1.000	1.000	1.000	1.000	1.000	1.000	1.000	1.000	0.950	1.000	1.000	1.000	0.857	1.000	1.000	1.000	0.900	0.150	1.000	1.000	1.000
c	–	–	–	–	–	–	–	–	–	–	0.050	–	–	–	–	–	–	–	0.100	0.850	–	–	–
LA1																							
a	–	1.000	1.000	0.875	0.667	1.000	1.000	1.000	1.000	1.000	1.000	1.000	–	–	–	–	–	–	–	–	–	–	–
b	–	–	–	0.125	0.333	–	–	–	–	–	–	–	–	–	–	–	–	–	–	–	–	–	–
c	1.000	–	–	–	–	–	–	–	–	–	–	–	1.000	1.000	1.000	1.000	1.000	1.000	1.000	1.000	1.000	1.000	1.000
LA2																							
a	1.000	1.000	1.000	1.000	1.000	1.000	1.000	1.000	1.000	1.000	1.000	1.000	1.000	1.000	1.000	0.650	1.000	1.000	1.000	1.000	1.000	1.000	1.000
b	–	–	–	–	–	–	–	–	–	–	–	–	–	–	–	0.350	–	–	–	–	–	–	–
LGG																							
a	–	–	–	–	–	–	–	–	–	–	0.100	–	–	–	–	–	–	0.556	–	–	–	–	–
b	1.000	1.000	1.000	1.000	1.000	1.000	1.000	1.000	1.000	1.000	0.900	1.000	1.000	1.000	1.000	1.000	1.000	0.444	1.000	1.000	1.000	1.000	1.000
MDH1																							
a	–	–	–	–	–	–	–	–	–	–	0.100	–	–	–	–	–	–	–	–	–	–	–	–
b	–	–	–	–	–	–	–	–	–	–	–	–	–	–	–	–	–	–	–	–	–	–	0.100
c	1.000	1.000	1.000	1.000	1.000	1.000	1.000	1.000	1.000	1.000	0.900	1.000	1.000	1.000	1.000	1.000	1.000	1.000	1.000	1.000	1.000	1.000	0.900

NADH1																								
a	–	–	–	–	–	–	–	0.050	0.100	–	–	–	–	–	–	–	–	–	–	–	–	–	–	–
b	1.000	1.000	1.000	1.000	1.000	1.000	1.000	0.950	0.800	1.000	1.000	1.000	1.000	0.100	0.100	1.000	0.800	1.000	1.000	1.000	1.000	1.000	1.000	1.000
c	–	–	–	–	–	–	–	–	0.100	–	–	–	–	–	–	–	0.200	–	–	–	–	–	–	–
d	–	–	–	–	–	–	–	–	–	–	–	–	–	0.900	0.900	–	–	–	–	–	–	–	–	–
PAP																								
a	–	–	–	–	–	–	–	–	–	–	–	–	–	–	–	–	–	–	–	0.222	–	–	–	–
b	0.900	0.375	1.000	0.938	0.833	1.000	0.450	1.000	0.900	0.750	0.500	1.000	1.000	1.000	1.000	1.000	1.000	1.000	1.000	0.778	–	0.500		
c	0.100	0.625	–	0.062	0.167	–	0.550	–	0.100	0.250	0.500	–	–	–	–	–	–	–	–	–	1.000	0.500		
PGD																								
a	0.500	–	–	–	–	–	–	0.300	–	–	0.100	0.200	–	–	–	–	–	0.100	0.500	0.500	0.500	0.500		
b	0.500	0.125	0.167	0.125	0.333	1.000	1.000	0.700	1.000	1.000	0.900	0.800	1.000	1.000	1.000	1.000	1.000	0.450	–	–	–	–		
c	–	0.875	0.833	0.875	0.667	–	–	–	–	–	–	–	–	–	–	–	–	–	–	–	–	–		
d	–	–	–	–	–	–	–	–	–	–	–	–	–	–	–	–	–	0.450	0.500	0.500	0.500	0.500		
PGM																								
a	1.000	1.000	1.000	1.000	1.000	1.000	1.000	1.000	1.000	1.000	1.000	1.000	1.000	1.000	1.000	0.900	0.444	0.600	–	–	–	–		
b	–	–	–	–	–	–	–	–	–	–	0.100	–	–	–	–	0.100	0.556	0.400	1.000	1.000	1.000	1.000		
SOD																								
a	1.000	1.000	1.000	1.000	1.000	1.000	1.000	1.000	1.000	1.000	1.000	1.000	1.000	–	–	–	–	–	1.000	1.000	1.000	1.000		
b	–	–	–	–	–	–	–	–	–	–	–	–	–	1.000	1.000	1.000	1.000	1.000	–	–	–	–		
% loci polymorphic	4.4	8.9	4.4	13.3	11.1	2.2	4.4	4.4	2.2	8.9	20.0	4.4	2.2	0.0	2.2	11.1	8.9	13.3	8.9	6.7	6.7	4.4	8.9	
Heterozygosity																								
Observed	0.009	0.053	0.030	0.031	0.022	0.000	0.016	0.000	0.000	0.009	0.020	0.022	0.004	0.000	0.000	0.022	0.007	0.037	0.022	0.027	0.022	0.022	0.030	
(SE)	(0.006)	(0.029)	(0.023)	(0.023)	(0.016)	(0.000)	(0.016)	(0.000)	(0.000)	(0.005)	(0.012)	(0.022)	(0.004)	(0.000)	(0.000)	(0.014)	(0.007)	(0.022)	(0.018)	(0.022)	(0.022)	(0.022)	(0.023)	
Expected	0.017	0.035	0.021	0.039	0.055	0.012	0.023	0.020	0.012	0.020	0.046	0.020	0.004	0.000	0.006	0.038	0.031	0.056	0.032	0.026	0.030	0.025	0.039	
(SE)	(0.013)	(0.018)	(0.015)	(0.017)	(0.024)	(0.012)	(0.016)	(0.014)	(0.012)	(0.012)	(0.016)	(0.015)	(0.004)	(0.000)	(0.006)	(0.018)	(0.016)	(0.022)	(0.016)	(0.016)	(0.017)	(0.018)	(0.020)	

Invariable loci: *AAT2, ADA1, ADH2, AK, ALDH, ALDO, CK, EST1, ESTD, G3PHD, G6PD, GDH, GLUD, HADH, LDH1, LDH2, ME, MDH2, MP1, NADH2, ODH, SORD, XDH.*